Available online at www.HighTechJournal.org

HighTech and Innovation Journal

ISSN: 2723-9535

Vol. 4, No. 2, June, 2023

Physicochemical and Microstructural Characterization of Klias Peat, Lumadan POFA, and GGBFS for Geopolymer Based Soil Stabilization

Adriana E. Amaludin [1], Hidayati Asrah [1, 2*], Habib M. Mohamad [1, 2*], Hassanel Z. bin Amaludin [3], Nazrein A. bin Amaludin [4]

[1] *Faculty of Engineering, Universiti Malaysia Sabah, Jalan UMS, 88400 Kota Kinabalu, Sabah, Malaysia.*

[2] *Green Materials and Advanced Construction Technology (GMACT) Research Unit, Faculty of Engineering, Universiti Malaysia Sabah, Jalan UMS, 88400 Kota Kinabalu, Sabah, Malaysia.*

[3] *Engineering Materials and Structures (eMast) iKohza, Malaysia-Japan International Institute of Technology, UTM Kuala Lumpur, Kuala Lumpur, 54100, Federal Territory of Kuala Lumpur, Malaysia.*

[4] *Centre of Research in Energy and Advanced Materials (CREAM), Faculty of Engineering, Universiti Malaysia Sabah, Jalan UMS, Kota Kinabalu, 88400, Sabah, Malaysia.*

Received 05 January 2023; Revised 26 April 2023; Accepted 14 May 2023; Published 01 June 2023

Abstract

Peat soils are highly heterogeneous and considered problematic because they have a high moisture content and low shear strength. It requires stabilization to enhance its engineering properties before it is transformed into a viable construction material. The use of geopolymers as stabilizer materials for weak soils has been on the rise recently due to their low carbon footprint compared to the use of conventional stabilizer materials like cement. Geopolymerization occurs as a result of the alkali activation of aluminosilicate materials. In this study, peat soil and the aluminosilicate materials Palm Oil Fuel Ash (POFA) and Ground Granulated Blast Furnace Slag (GGBFS) are characterized to assess their suitability as geopolymer precursor materials. A series of laboratory studies were carried out to determine the physicochemical properties of the materials, such as particle size distribution, moisture and organic content, specific gravity, pH, and electrical conductivity. Furthermore, the XRD, XRF, and FESEM tests were carried out to ascertain the mineral characteristics, elemental chemical composition, and morphological characteristics of these materials, respectively. The peat soil is classified as hemic peat with sufficient aluminosilicate content (Si/Al ratio of 2.11). The POFA is identified as Class F pozzolan with adequate Si+Al+Fe oxide content (67.9%), as stipulated by ASTM C618. The GGBFS material was found to be appropriate for geopolymer production, with a Si/Al ratio of 2.17, a hydration modulus of 2.38 (good hydration), and a basicity coefficient of 1.32 (alkaline material favorable for geopolymerization). Based on the geopolymer precursor material suitability assessment criteria, all the materials assessed were deemed suitable for geopolymerization, and the effectiveness of POFA-GGBFS geopolymer to improve peat soil properties should be studied in depth. At present, there are limited studies pertaining to the use of alkali-activated POFA-GGBFS blends to improve peat soil properties. As a result of this material characterization phase, planned works involving the compressive strength testing program on alkali-activated POFA-GGBFS-peat soil blends at ambient temperature will be carried out in the near future. The eventual aim of this research is to remediate the peat soil to be repurposed as road subgrade material.

Keywords: Geopolymer; Peat Soil; Palm Oil Fuel Ash; Ground Granulated Blast Furnace Slag; Material Characterisation.

* Corresponding author: hidayati@ums.edu.my; habibmusa@ums.edu.my

http://dx.doi.org/10.28991/HIJ-2023-04-02-07

1. Introduction

Peat soils are defined as highly heterogeneous materials, as they are derived from decomposing organic matter, i.e., plant leaves and roots, and are typically brown or black in color [1]. Peat soil is considered a problematic soil because it has a high natural moisture content and low shear strength [2]. The problems associated with peat soils should be resolved by means of soil stabilization. Nicholson [3] defines chemical stabilization as a technique applied to enhance the engineering characteristics of problematic soils, i.e., to increase the soil shear strength where stabilizing binders are mixed with weak soils found on site. This research work is focused on the use of geopolymers to improve the engineering properties of weak soils.

Geopolymer materials are created from the combination of two precursor materials, namely aluminosilicate materials (e.g., fly ash and ground granulated blast furnace slag), and highly alkaline solutions to activate the precursor materials. In most cases, geopolymer materials are used to improve the strength of mortar and concrete [4, 5]. More recently, the use of agricultural and industrial waste-derived geopolymer materials as soil stabilizers has been applied in the geotechnical field, with published studies reporting on the enhancement of engineering properties and improved durability of weak soils [6, 7]. Various types of geopolymer source materials were used for soil stabilization purposes, such as coffee grounds [8], tea wastes [9], fly ash [10, 11], GGBFS [6, 12], and POFA [13–15]. In the context of this study, the outcomes of selected studies conducted on POFA-based geopolymers used as construction and weak soil stabilizer materials are discussed below.

It is important to note that geopolymer synthesis for soil stabilization must take place under ambient temperature conditions to emulate the conditions on site. In contrast, most of the existing studies on the strength of geopolymer materials are conducted at elevated temperatures, achieved by subjecting the material to oven curing for 24 hours and subsequently cured at ambient temperature. For example, the study by Yahya et al. [16] discovered that POFA geopolymers cured at ambient temperature produced the lowest compressive strength at 0.4 MPa, while the highest compressive strength (11.5 MPa) was achieved at 80°C oven curing. More recently, the findings of Kwek et al. [17], which focused on POFA geopolymers synthesized at ambient temperature, showed that the 28-day compressive strength of 21.31 MPa is achievable with the appropriate amount of alkaline activator and adequate metal oxides contained in the source material. The results of these studies show that POFA geopolymer is a viable source material for creating geopolymers with adequate strength.

On the other hand, the existing studies on the use of POFA-based geopolymer materials are very limited, and the outcome of these studies has been discussed in depth in a recent review paper [18]. In the study conducted by Zainuddin et al. [15], POFA geopolymer was used as a soil stabilizer for weak laterite soil. They reported that the strength of laterite soil improved from 106 kPa to 340 kPa after 7 days of curing, with a 15% POFA geopolymer content. Meanwhile, the research carried out by Khasib et al. [14] examined the effect of adding POFA geopolymer on the strength of low- and high-plasticity clays. The unconfined compressive strength (UCS) value for the low-plasticity clay improved from 260 kPa to 4180 kPa, while the UCS value for the high-plasticity clay improved from 130 kPa to 2860 kPa after 28 days of curing. Lastly, the findings reported by Abdeldjouad et al. [13] showed that POFA geopolymer treatment was effective for low plasticity silt and high plasticity clay, where the soil UCS at 28 days of curing was valued at 1930 kPa for the silt and 1320 kPa for the clay. In these studies, it is imperative that an alkaline solution of adequate molarity is used to dissolve the alumina and silica contents in the soil-aluminosilicate-alkaline mix to form the soil-geopolymer matrix [19]. This is because geopolymer source materials that were not activated by the alkaline solution adversely impact the soil-geopolymer specimen strength since they act as filler materials, as stated by Pourakbar et al. [20]. As such, in order for the POFA geopolymer to effectively stabilize the weak soil, it should consist of substantial amounts of aluminates and silicates to facilitate the pozzolanic reactions that enable the soil stabilization process to occur. The results from these studies utilizing POFA geopolymer as a soil stabilizer demonstrate that this material can be used to treat other types of weak soils, such as fibric, hemic, and sapric peat soils. In addition, the outcome of the review conducted by Amaludin et al. [18] stated that the attempt to synthesize POFA and GGBFS geopolymers for soil stabilization purposes has not yet been established.

In the following sections, the material preparation and characterization tests for Klias peat and the aluminosilicate materials (POFA and GGBFS) are explained in detail. A series of laboratory studies were designed to determine the physicochemical properties of the materials. Furthermore, the XRD, XRF, and FESEM tests were carried out to ascertain the mineral characteristics, elemental chemical composition, and morphological characteristics of these materials, respectively. These tests were carried out to determine the suitability of the said materials as geopolymer source materials, based on the metal oxide requirements of ASTM C618 [21] and ACI Committee 233R-17 [22], and the criteria defined by Ghosh & Ghosh [23], with additional references made to book chapters published by Garcia-Lodeiro et al. [24] and Manjunath & Narasimhan [25] on the advances of alkali activated binders. The in-depth discussion on the geopolymer source suitability check is discussed further in Section 4.5: Geopolymer Precursor Material Suitability Assessment.

Therefore, the objective of this study is to establish the physicochemical, chemical composition, mineralogy, and morphology characteristics of Klias peat soil, Lumadan Palm Oil Fuel Ash (POFA), and Ground Granulated Blast Furnace Slag (GGBFS). From the acquired characterization test results, the salient parameters will be used to assess the suitability of the aforementioned materials as geopolymer precursors. Figure 1 shows the flowchart of the research

conducted in this study. Subsequently, the other parameters established in this characterization study are used to detect the changes in the physicochemical, chemical composition, mineralogy, and morphology characteristics of the peat, POFA, and GGBFS when all three materials are activated with alkali to create a POFA-GGBFS-soil geopolymer matrix. The findings presented in this paper are part of ongoing research that focuses on the application of alkali-activated POFA-GGBFS blends to improve the shear strength of Klias peat soil.

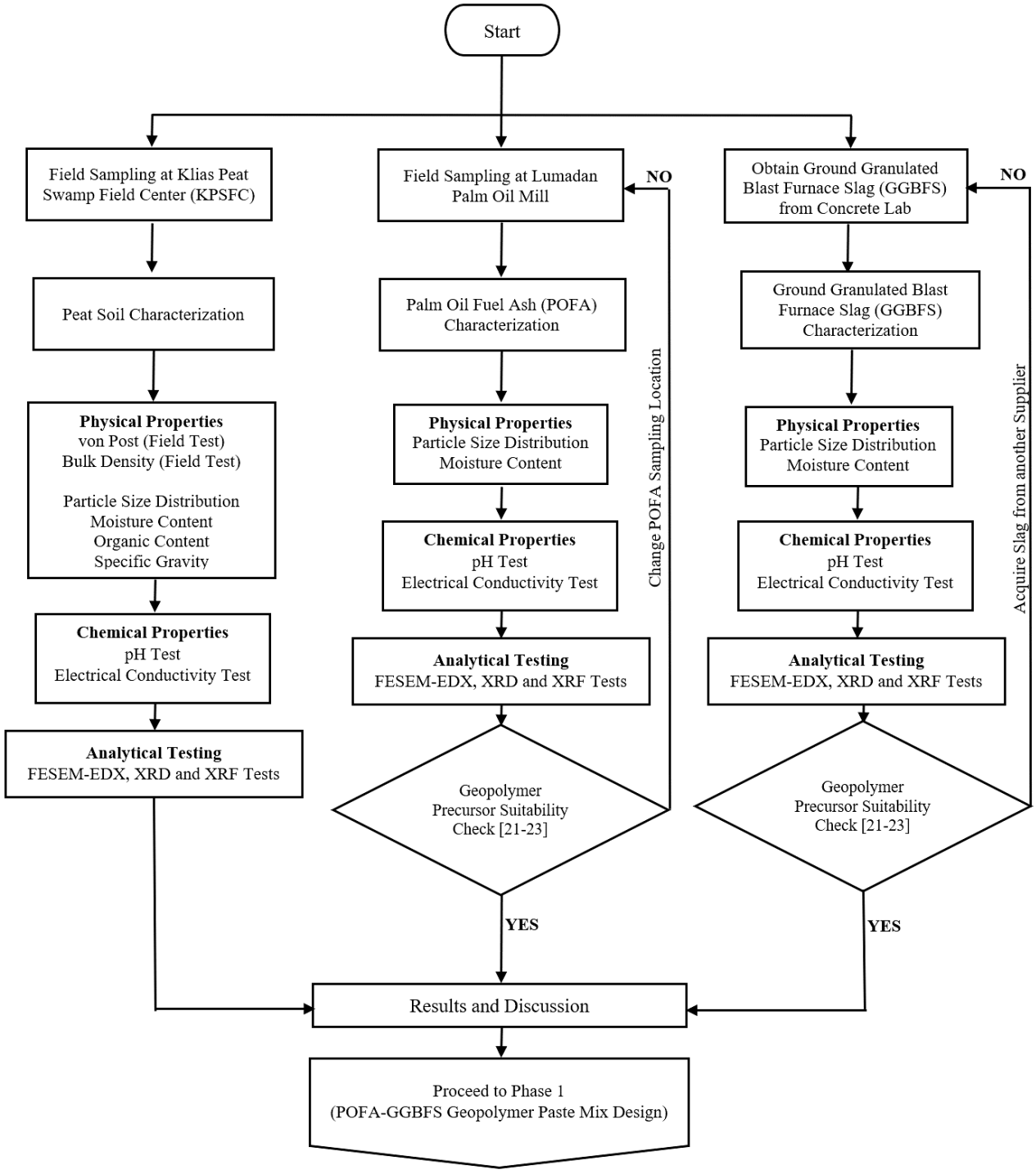

Figure 1. Research flowchart for this study

2. Materials

2.1. Klias Peat Soil

In April 2022, around 80 kg of Klias peat soil was obtained from a palm oil plantation area bordering the Klias Peat Swamp Field Centre (KPSFC), Beaufort, Sabah, Malaysia (coordinates: 5° 19.571' N, 115° 40.363' E), as shown in Figure 2. The peat samples were obtained from a depth of 0–0.3 m, since the ground water table (GWT) was located at

0.34 m beneath the soil surface [26]. The peat samples were sealed in polythene bags to preserve their natural moisture content and were subsequently transported to the Geotechnical Engineering laboratory, Block E, Faculty of Engineering, UMS. Figures 3-a to 3-c show the site coordinates near KPSFC, the GWT measurement, and the peat sampling site, respectively. The collected samples were classified as disturbed samples and were air-dried for 24 hours at an ambient temperature of 30 ± 3°C with adequate ventilation before being oven-dried for another 24 hours at 100 ± 5°C to ensure that the soil was dried to a constant weight. The oven-dried soil was then sieved with a 2-mm sieve opening to produce the samples required for the soil characterization tests. An array of characterization tests were conducted, such as particle size distribution, natural moisture content and organic content, specific gravity, pH, and electrical conductivity tests. Meanwhile, several tests were conducted on site, such as the von Post test and the bulk density test. A detailed explanation of these in-situ and laboratory tests will be covered in Section 3: Experimental Methodology, while the physicochemical properties of the peat soil will be presented in Section 4: Results and Discussion.

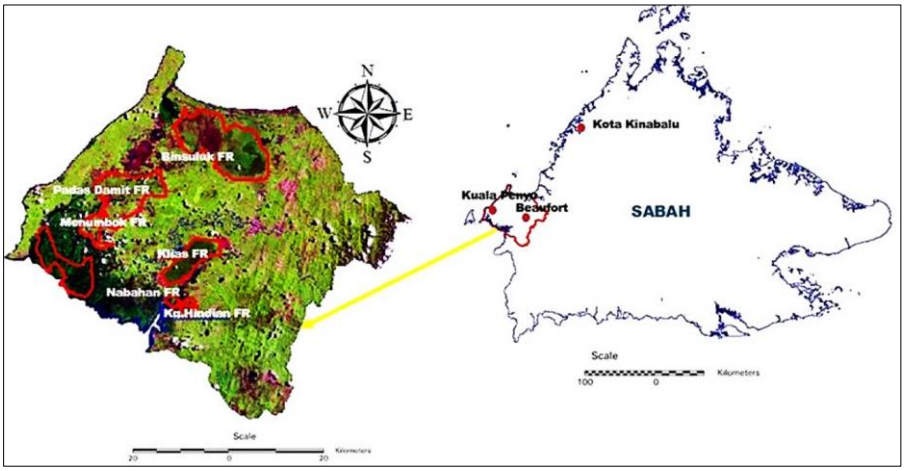

Figure 2. Location of Klias Peat Swamp Field Centre (KPSFC), Beaufort, Sabah, Malaysia

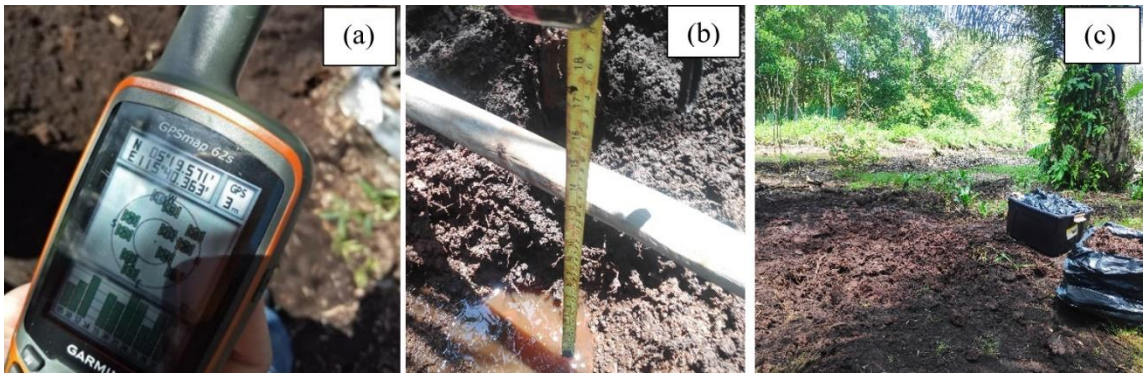

Figure 3. (a) Site coordinates; (b) GWT at 0.34m depth; (c) Peat sampling site

2.2. Lumadan Palm Oil Fuel Ash (POFA)

For this study, around 50 kg of POFA material was collected from Lumadan Palm Oil Mill, Beaufort (courtesy of Sawit Kinabalu Sdn. Bhd.) in the month of April 2022, which will be used as a geopolymer source material. This material was previously used in studies conducted by Asrah et al. [27] and Tonduba et al. [28] for the production of POFA-based mortar and bricks, and the material was classified as a Class C pozzolan based on the ASTM C618-19 standard based on the sum of its major oxides [21]. The classification of the POFA material used in this study will be discussed further in Section 4.2, which will compare the findings of this study with the results of previous studies. Unprocessed or raw POFA obtained from the palm oil mill is not suitable for direct use as geopolymer precursor material since it still contains much unburned residue, as evidenced by its elevated value of loss on ignition (LOI), as reported by Asrah et al. [27]. Furthermore, since the POFA material is derived from burning palm oil waste materials in a boiler machine [29], the partially ashed agricultural waste contains debris material that should be sieved and treated before it is used as a stabilizer material. The process of treating unprocessed POFA into pre-treated POFA (oven dried for 24 hours at 100 ± 5°C and sieved with a 300 mm sieve) was done as recommended by previous researchers to ensure that the material is free from moisture prior to its use as a geopolymer precursor material [20, 30, 31]. Subsequently, the dried and sieved POFA (otherwise known as pre-treated POFA) were collected and subjected to mechanical activation using a planetary grinding ball mill.

Approximately 600 g of POFA was ground with the ball mill for three (3) hours at 300 rpm to produce ground POFA, as recommended by Tonduba et al. [32]. Figure 4 illustrates the process of treating the raw POFA to create ground POFA for the purpose of geopolymerization.

Figure 4. Processing raw POFA to produce ground POFA

2.3. Ground Granulated Blast Furnace Slag (GGBFS)

Ground Granulated Blast Furnace Slag (GGBFS) is a material derived from steel and iron manufacturing, mainly comprising calcium oxide, silica, and aluminum oxide [23]. In recent times, the use of GGBFS as supplementary cementitious material (SCM) has seen an uptick across the construction industry due to its high content of calcium and silicon oxides that enhance the cementation process and are considered a viable material for engineering applications [33]. The GGBFS used in this study was sourced from the Concrete Laboratory, Faculty of Engineering, Universiti Malaysia Sabah. In the aspect of geopolymer production, GGBFS is used to improve the production of POFA geopolymer at ambient temperature, as recommended by recent research findings that used fly ash-GGBFS mixtures to create geopolymers [11, 34].

3. Experimental Methodology

The current study focuses on establishing the physicochemical, mineralogy, and morphology characteristics of Klias peat, Lumadan POFA, and GGBFS materials. It was designed based on the existing engineering standards, such as ISO 13320: 2020 for laser particle size distribution, BS1377: Part 2 for soil moisture content and organic content, and ASTM D2976-22 for pH and electrical conductivity. Furthermore, for the analytical studies, the X-ray Diffraction (XRD) test was conducted for mineral characterization, the X-ray Fluorescence (XRF) test was conducted for the purpose of chemical composition characterization, and lastly, the Field Emission Scanning Electron Microscopy (FESEM) test was carried out to define the morphology characteristics of the materials. The research flowchart for this study was presented previously in Figure 1.

3.1. Particle Size Distribution

The particle size distribution (PSD) characterization was determined using a laser diffraction particle size analyzer (Model: Shimadzu SALD-2300), available in the Analytical Laboratory, Malaysia-Japan International Institute of Technology (MJIIT), Universiti Teknologi Malaysia, Kuala Lumpur. The peat soil, POFA, and GGBFS samples were sent to the analytical laboratory to ascertain their PSD characteristics, and the tests were carried out based on the ISO 13320: 2020 [35] standard. According to Arvaniti et al. [36], the Laser Diffraction (LD) method was able to characterize the full PSD, specifically via the measurement of light scattered by the particles subjected to the test. The two optical models used to convert the light scattering data to PSD are the Fraunhofer diffraction model and the Mie theory. In this study, the Mie theory was chosen because it is suitable for materials with small particles of ≤ 50 mm in size. To use Mie theory effectively, the optical properties, i.e., refractive index and absorption index, were provided to the LD machine technicians to ensure that the PSD results for the peat, POFA, and GGBFS samples were correctly reported. The works of Arvaniti et al. [36] and Cyr and Tagnit-Hamou [37] were instrumental in the selection of the values for refractive and absorption indices used in this study, as both studies focused on the optical properties of cementitious materials. Table 1 shows the refractive and absorption indices used for the LD measurement and the corresponding references for these values.

Table 1. Refractive and absorption indices for LD measurement of geopolymer materials

Material	Refractive index, *n*	Absorption index, *k*	Reference
Peat soil	1.52	0.1	Polakowski et al. [38]
Palm Oil Fuel Ash (POFA)	1.56	1.0	Jewell & Rathbone [39]
Ground Granulated Blast Furnace Slag (GGBFS)	1.62	0.1	Jewell & Rathbone [39]

3.2. Degree of Decomposition/ von Post Classification

This *in-situ* test is based on the von Post classification system [40]. Some peat soil was squeezed by hand until the water was drained from the soil. The extruded soil between the fingers was then subjected to a visual inspection by observing the amount of plant structure contained in the peat sample, indicating the degree of peat soil decomposition. The classification ranges from H_1-H_3 for fibric peat with an insignificant amount of decomposition, H_4-H_6 for hemic peat with moderate decomposition and indistinct plant structures, while H_7-H_{10} is designated for sapric peat that has undergone advanced decomposition. As a reference, the peat soil studied in this paper is hemic peat with moderate decomposition (H_4-H_6).

3.3. Natural Moisture Content and Organic Content

To determine the natural moisture content of peat soils, this analysis was carried out in accordance with BS 1377: Part 2: 1990: Clause 3.2 [41]. Peat soil of approximately 30 g was placed in empty crucibles and placed in an oven set at 105 ± 5°C for 24 hours. The natural moisture content was then obtained by dividing the amount of moisture loss by the weight of the oven-dried peat soil.

The organic content of peat soils was determined by taking the remains of the natural moisture content test specimens and burning the oven-dried peat specimens in a muffle furnace at 550°C for 5 hours. This test was carried out based on BS 1377: Part 3: 1990: Clause 4.0 [42]. First, the ash content (AC) is acquired, which is the weight of soil after it was ashed in the furnace. Subsequently, the organic content is calculated by subtracting the value of AC from 100%.

O'Kelly [43] stated that for peat and organic soils, the measurements obtained from a series of laboratory tests, i.e., natural moisture content, organic content, and its degree of decomposition, are more appropriate parameters to reflect the geoengineering behavior of organic soils. Typical soil index properties such as liquid limit and plastic limit (or consistency limits) are unsuitable for organic soils and better suited for clayey or silty soils. This is because many correlations have been made between the peat natural moisture content and the organic content, von Post classification, and bulk density of peat soils [44].

3.4. Bulk Density and Specific Gravity

During the site visit, the bulk density of the peat soil was determined on site using the Core Cutter method, as stipulated in BS 1377: Part 9: Clause 2.4 [45]. The core cutter is a steel cylinder with a 10 cm diameter and 12.7 cm height. It was driven into the ground using a 9 kg rammer. While the rammer is used to push the core cutter into the ground, a steel dolly with a 2.5 cm height is placed on top of the cutter to avoid any distortion to the core cutter. The bulk density is calculated by dividing the weight of soil contained in the cutter by its volume. Figure 5-a shows the driving rammer, 5-b shows the core cutter and steel dolly, and 5-c shows the core cutter driven into the ground, respectively.

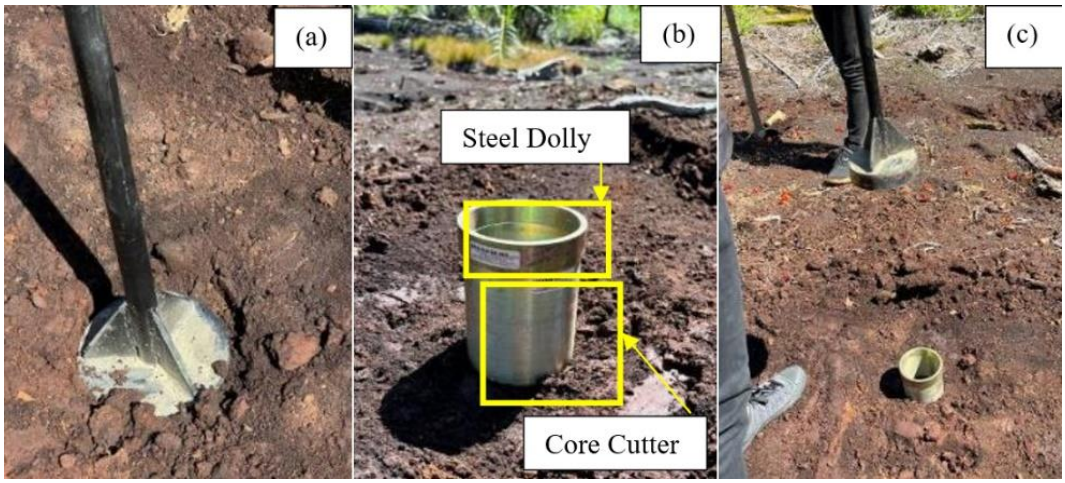

Figure 5. (a) Driving rammer; (b) Core cutter and steel dolly; (c) Core cutter driven into peat soil

Specific gravity is the ratio of the density of a material with reference to the density of water (Specific Gravity, G_s of Water is 1.00). To determine the specific gravity of peat, the tests were conducted based on BS 1377: Part 2: 1990 [41], but instead of using water, kerosene is used since the specific gravity of peat soils is typically lower than water. With 10 g of oven-dried peat specimens (passing a 425 mm sieve), the soil specific gravity was determined using a 50 ml pycnometer bottle, and triplicate samples were made to obtain the average reading.

3.5. pH and Electrical Conductivity

The pH (potential hydrogen) value of the peat, POFA, and GGBFS material is a crucial parameter to be established in this study since the soil stabilization process involves the ionic interactions between the soil and the stabilizer material. Based on ASTM D2976-22 [46], the pH value is obtained by weighing 3 g of the material and diluting it with 50 ml of ultrapure water [47] inside a 100 ml beaker, where it was soaked with occasional stirring at 180 rpm for 30 minutes. The pH measurement was carried out using a HANNA HI9810302 HALO2 GroLine pH meter. Subsequently, electrical conductivity (EC) measures the ability of a material to conduct electricity, measured in microSiemens per cm (μS/cm). Using the same solution prepared for the pH measurement, the EC of the peat soil and POFA material were measured using the HANNA HI98331 GroLine EC meter. The EC reading indicates the amount of calcium and hydroxyl ions available for the pozzolanic reaction between soil particles and stabilizer materials. The pH and EC meters were calibrated according to the manufacturer's standards before the commencement of both tests.

3.6. X-Ray Diffraction (XRD)

The X-ray diffraction (XRD) testing was performed with the Rigaku SmartLab X-ray diffractometer. XRD testing is a type of non-destructive chemical analysis of materials done with samples prepared in the form of a thin film or powder. Establishing the crystal structure and orientation, phase identification, and detection of trace chemicals in a sample can all be carried out with the XRD test. In the event that the layers of atoms in a crystalline mineral scatter the X-rays of a given wavelength, the diffraction of the rays will create a pattern of peaks that are unique to the mineral [48, 49]. More specifically, the vertical scale (peak height) of an XRD pattern represents the intensity of the diffracted ray, while the horizontal scale (diffraction angle) gives an indication of the crystal lattice spacing.

For this study, the XRD analysis was conducted with Cu-Kα radiation using the following equipment settings: 40 kV tube voltage and 35 mA current. Subsequently, the XRD patterns were acquired using a sweep between 3° to 80° at a rate of 1° (2θ) per minute and a 0.01° step size. The results of the test were compared to the International Centre for Diffraction Data (ICDD) database [50].

3.7. X-Ray Fluorescence (XRF)

In order to establish the chemical composition of the peat, POFA, and GGBFS materials, the X-ray fluorescence (XRF) test was carried out. According to Yusuf [51], the XRF test starts with the material being irradiated with a primary X-ray beam from a radioisotope, causing the electron from the sample to be dislodged. After the irradiated material has stabilized, it will emit fluorescent X-rays, and this fluorescent X-ray energy released by the material can therefore be measured to quantify the chemical composition of a given material.

The XRF test was carried out using the XRF machine (Model: Malvern Panalytical Epsilon 1), located in MJIIT, UTM Kuala Lumpur. The peat, POFA, and GGBFS samples (passing 75 mm and weighing 10 g each) were sent to the analytical laboratory to ascertain their chemical composition, and the tests were carried out based on the ASTM E1621-21 standard [52]. Results obtained from this test will determine if the chosen POFA and GGBFS materials possess adequate metal oxides, as required by the ASTM C618-19 standard, which states that the total metal oxides (SiO_2, Al_2O_3, Fe_2O_3) should amount to at least 50% [21].

3.8. Field Emission Scanning Electron Microscopy (FESEM)

The Field Emission Scanning Electron Micrograph (FESEM) tests have been carried out to analyze the morphological characteristics of the peat, POFA, and GGBFS materials. A scanning electron microscope (SEM) allows the researcher to obtain the material surface texture morphology [53], specifically using incident electron beams that are scanned in a raster pattern across the sample surface, and the backscattered or emission of secondary electrons is then identified [54]. Additionally, the term field-emission (FE)-SEM refers to the use of a high-energy electrical field to emit electrons with a cathode called a field emitter [54], which strikes the material to produce magnified images as a result of the electron-material interaction. The testing procedure was carried out as specified in the ASTM E986-04 standard [55].

Prior to testing, the specimen was thoroughly dried and coated with a conductive material using a sputter coater machine (Model: JEOL JEC-3000FC). The conductive material chosen was platinum powder because the gold coating used in normal SEM is too coarse and could hide the morphological features seen in the ultra-high-resolution images produced by the FESEM machine [56]. In the sputter coater, the platinum powder was spread evenly onto the specimen

surface using a vacuum chamber containing argon gas. The electrical charges induced within the chamber cause the platinum coating to form on the surface of the sample [57]. After undergoing sufficient coating, the sample was then placed inside the JEOL JSM-7900F FESEM machine to characterize the morphological data of the peat soil, POFA, and GGBFS particles.

4. Results and Discussion

4.1. Physical Properties

The physicochemical properties of Klias peat soil are presented in Table 2, and comparisons were made between the results obtained in this study and past research findings. According to the Particle Size Distribution (PSD) test, it was found that the peat soil consists of 41.1% coarse-grained material, while the fine-grained material amounted to 58.9%, and the mean particle size (d_{50}) was found to be 55.48 µm. The PSD graph for Klias peat is shown in Figure 6.

Table 2. Physicochemical properties of Klias peat and hemic peat in past studies

	Physicochemical properties	Unit	Engineering standard	Present study	Mohamad et al. [58]	Paul & Hussain [61]
Particle Size Distribution	Coarse Grained	%	ISO 13320: 2020 (Laser Diffraction) [35]	41.1	-	-
	Fine Grained (< 75 µm)	%		58.9	-	-
	d_{50}	µm		55.48	-	-
	Degree of Decomposition	-	von Post criteria [40]	Hemic (H_6)	Hemic (H_6)	Hemic (H_5-H_7)
	Natural Moisture Content	%	BS 1377: Part 2: Cl. 3.2 [41]	657	682	404
	Organic Content	%	BS 1377: Part 3: Cl. 4.0 [42]	96.57	98.43	76
	Bulk Density	g/cm^3	BS 1377: Part 9: Cl. 2.4 [45]	1.01	-	1.15
	Specific Gravity	-	BS 1377: Part 2: Cl. 8.3 [41]	1.68	1.42	1.22
	pH	-	ASTM D2976-22 [46]	3.42	4.25	4.5
	Electrical Conductivity	µS/cm	ASTM D2976-22 [46]	201	-	333

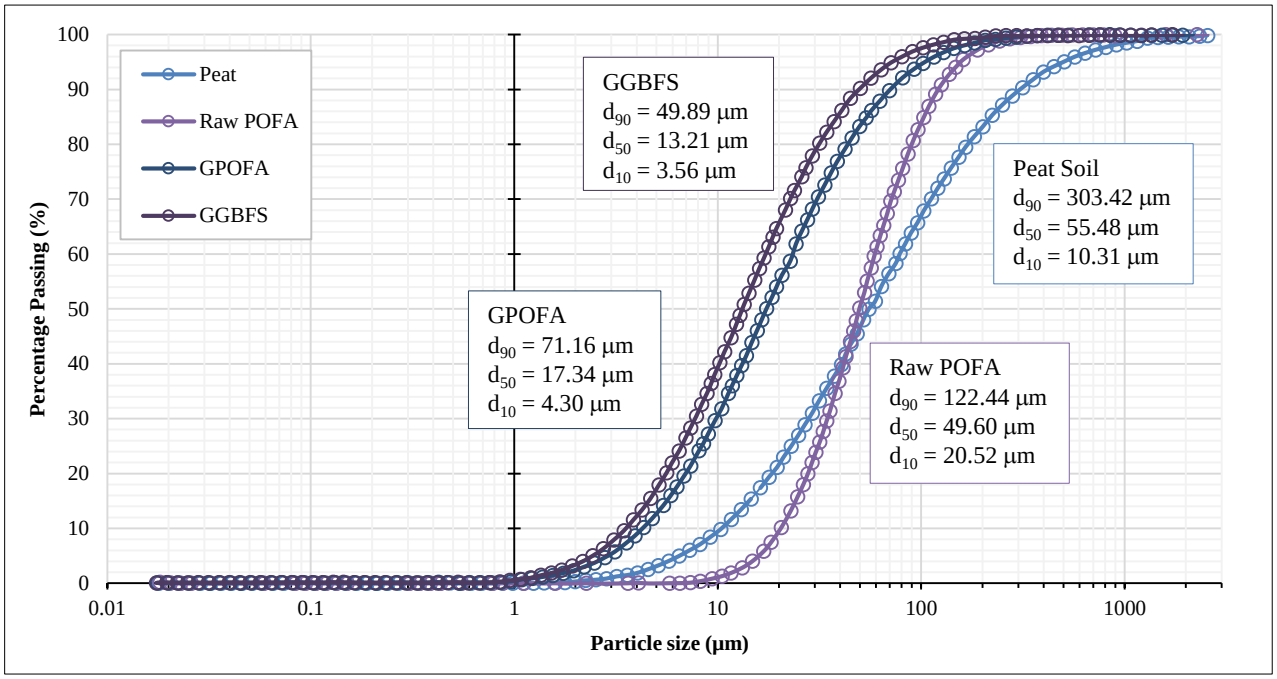

Figure 6. Particle size distribution of Klias peat, raw POFA, GPOFA, and GGBFS

Additionally, based on the von Post criteria, the Klias peat soil was classified as hemic peat (H_6). The natural moisture content obtained was 657%, within the range of previously published values for peat originating from Klias, Beaufort, and Sabah [58, 59]. The organic content was valued at 96.57%, and conventional values of organic content for peat soils from East Malaysia are within the range of 50–98% [1]. It seems that the natural moisture content can be correlated with its organic content, where peats with organic contents are directly proportional to their natural moisture content, as seen with the low moisture content recorded for Indian peat at 404% moisture content with 76% organic content, as reported by Paul and Hussain [60]. The bulk density of Klias peat was valued at 1.01 g/cm^3, which is slightly less dense compared

to Indian hemic soil at 1.15 g/cm^3 [61]. This is because Huat et al. [1] stated that the bulk density of peat can be correlated to its von Post classification, where a higher decomposition of peat results in a higher bulk density. More specifically, Klias peat is classified as hemic (H_6) while the Indian peat is classified as hemic (H_7) with a higher level of decomposition; therefore, this corresponds to the higher bulk density value of the Indian peat with a value of 1.15 g/cm^3, as previously mentioned. The specific gravity value of Klias peat was determined to be 1.68, which is relatively high compared to the findings of Mohamad et al. [58] and Paul & Hussain [61], with values ranging between 1.37-1.42. According to Huat et al. [1], higher specific gravity indicates the presence of higher mineral contents, and this will be discussed further in Section 4.2: Mineral Characteristics (XRD).

Subsequently, the pH and EC tests were also performed on Klias peat soil. For the pH value of Klias peat, it was found that the pH 3.02 value is slightly more acidic than the values found in previous studies by Mohamad et al. [58] and Paul & Hussain [61]. However, the author's findings are similar to the findings of [59] with pH 3, and the pH value of 3.6 reported by Lau et al. [62] for Irish Hemic Bog Peat. Furthermore, Huat et al. [1] stated that the typical pH value for tropical peat is within the range of pH 3–4. Therefore, Klias peat can be classified as highly acidic peat, as stipulated by ASTM D2976-22 [46]. Soils with organic acids possessing pH values below 9 are detrimental to the formation of cementitious products [63], which interferes with the soil stabilization mechanism, and therefore the acidic nature of peat soil must be balanced with the alkalinity from the geopolymer source materials, i.e., POFA and GGBFS.

In the case of EC, this parameter for peat soil has recently been reported by researchers working on peat soils [12, 61]. For Klias peat, the EC value was found to be 201 µS/cm, while for the Indian hemic peat, the EC value was 333 µS/cm [61]. It was suggested by Khanday et al. [12] that the value of EC is inversely proportional to its organic content, with higher organic content peats yielding lower values of EC. Klias peat has an EC value of 201 µS/cm with 96.57% organic content, while Indian peat has an EC value of 333 µS/cm at 76% organic content; therefore, the correlation proposed by Khanday et al. [12] can be applied to the findings of the current research. In addition, Paul and Hussain [64] concluded in their study that EC values in peat soils are directly correlated to the value of pH, where higher pH values (more alkaline material) produce higher values of EC. For instance, the EC value for Klias peat at 201 µS/cm has a pH value of 3.42, while the EC value of Indian peat at 333 µS/cm has a higher pH value of 4.5, and both studies are in agreement with the conclusion made by Paul and Hussain [64].

Table 3 shows the physicochemical properties of the chosen geopolymer precursor materials: raw palm oil fuel ash (POFA), ground POFA (GPOFA), and ground granulated blast furnace slag (GGBFS). As mentioned previously, the PSD of the geopolymer precursor materials was measured with a laser particle size analyzer, and the resulting PSD graph is shown in Figure 6, with the mean particle size (d_{50}) for raw POFA, GPOFA, and GGBFS being 49.6, 17.33, and 13.21 mm, respectively. With a d_{50} value of 17.33 mm for the GPOFA, it is classified as a medium-sized POFA [27] and does not fall under the ultrafine category [28]. Similar sizes for GPOFA were reported by Khalid et al. [65] with a mean particle size (d_{50}) of 14.21 mm, while Kroehong et al. [66] reported the d_{50} of GPOFA as 15.6 mm, and Lim et al. [67] stated that the d_{50} of GPOFA was 14.58 mm. It is apparent that the mechanical activation by grinding had managed to reduce the mean particle size of the POFA by 65%. This resulted in a higher percentage of fine-grained material for GPOFA, where 90.98% of the sample had passed the 75-mm sieve. Based on ASTM C618-19, the allowable percentage of particles finer than 45 mm for fly ash material is 34% at most. From Table 3, it is apparent that raw POFA with 54.9% retention on a 45-mm sieve is classified as "off-specification" since the limit is set at 34% [21]. Therefore, after the mechanical activation, the GPOFA had a 19.2% retention on the 45-mm sieve and is therefore acceptable to be used as calcined natural pozzolan.

Table 3. Physicochemical properties of raw POFA, ground POFA and GGBFS

	Physicochemical properties	Unit	Raw POFA	Ground POFA	Ultrafine POFA [28]	GGBFS	GGBFS [12]
Particle Size Distribution	Coarse Grained	%	28.01	9.02	-	4.69	0
	Fine Grained (< 75 µm)	%	71.99	90.98	-	95.31	100.00
	d_{50}	µm	49.6	17.33	1.5	13.21	11.16
	Retained on 45 µm	%	54.9	19.2	-	11.7	3.0
	Natural Moisture Content	%	69.14	1.87	2.23	0.93	-
	pH	-	9.00	8.97	-	8.68	8.5
	Electrical Conductivity	µS/cm	658	405	-	996	-

According to Lim et al. [68], grinding the aluminosilicate material to a smaller size improves its pozzolanic activity. However, Ghosh and Ghosh [23] recommend that for the Class F fly ash material (with more amorphous content vs. Class C fly ash), the fineness of the fly ash should not be too high as more energy is required for the geopolymerization process. Ghosh and Ghosh [23] clarified that for alkali activation of fly ash at ambient temperatures on site, Class F fly ash with moderate fineness is most suitable, as heat curing *in-situ* is not a plausible solution. In addition, the effect of grinding POFA on its morphology will be discussed in Section 4.4.

On the other hand, for Ground Granulated Blast Furnace Slag (GGBFS), ASTM C989-09 states that the allowed amount of material passing the 45 μm sieve is 20% at most [69]. It can be seen from Table 3 that the chosen GGBFS material is within the specification stated in the said ASTM standard, with only 11.7% material retention on the 45 μm sieve. The mean particle size of the GGBFS used in this study is also comparable to the findings of Khanday et al. [12], where the d_{50} value for GGBFS originating from India was found to be 11.16 μm.

For the evaluation of the natural moisture content, the ASTM C618-19 standard applies to the POFA material as well. The requirement of maximum moisture content for materials according to ASTM C618-19 is at 3%, and for this study, it is apparent that the natural moisture content of raw POFA at 69.14% is "off-specification" and should be subjected to further treatment before it is used as a geopolymer precursor material. After treatment and grinding, the moisture content was valued at 1.87% and is compliant with the requirements of the ASTM standard. The value obtained for this study is also comparable to that obtained by Tonduba et al. [28], with a moisture content value of 2.23%. In the case of GGBFS, the moisture content was valued at 0.93%. Chesner et al. [70] stated that the presence of moisture in GGBFS due to the granulation process is a concern, and the moisture should be removed prior to its use. As such, care is taken to avoid any instances of moisture intrusion into the GGBFS by storing it in an airtight container.

Meanwhile, for the alkalinity assessment, raw POFA was valued at pH 9, for GPOFA the pH had dropped slightly to 8.97, and for GGBFS the pH value was found to be 8.68. The highly alkaline values for POFA and GGBFS are indicative of their ability to create an alkaline environment that is conducive to the dissolution of the aluminosilicate materials [61] and the production of geopolymeric compounds. Subsequently, for the EC values of the geopolymer precursor materials, raw POFA had an EC value of 658 μS/cm, GPOFA had an EC value of 405 μS/cm, and GGBFS had the highest EC value at 996 μS/cm. Shehata et al. [71], as cited by Dinakar et al. [72], stated that the EC value is determined by the composition of the pore solution, where fly ash materials with lower lime and alkali content (compared to Portland cement) resulted in lower concentrations of alkali ions and associated hydroxyl ions. This statement is in line with the findings of the current study, where the GPOFA produced a lower EC value because it was subjected to oven drying and therefore possessed a lower moisture content compared to raw POFA. For GGBFS, this material has a significant amount of lime (which will be discussed in Section 4.3), resulting in the highest EC value among the three geopolymer precursor materials, valued at 996 μS/cm. The GGBFS EC result is also in good agreement with the findings of Shehata et al. [71] and Dinakar et al. [72].

4.2. Phase Analysis and Mineral Characteristics (XRD)

Figure 7 shows the X-ray diffraction patterns for Klias peat, GPOFA, and GGBFS. For Klias peat, Figure 7-a shows that the major mineralogical component of the soil is quartz (SiO_2) (ICDD reference: 01-089-8936), with peaks detected at 2θ = 26.56°, 59.75°, and 68.1°. The presence of quartz in peats was also reported by Khanday et al. [12], Paul and Hussain [61], and Abdila et al. [73], although instances of other compounds such as kaolinite, calcite, and hydrated halloysite were not detected in this study. This occurrence of quartz, otherwise known as silicon oxide (SiO_2), was also seen in the X-ray fluorescence (XRF) results, amounting to 21.9% of the material compound, which will be further discussed in Section 4.3.

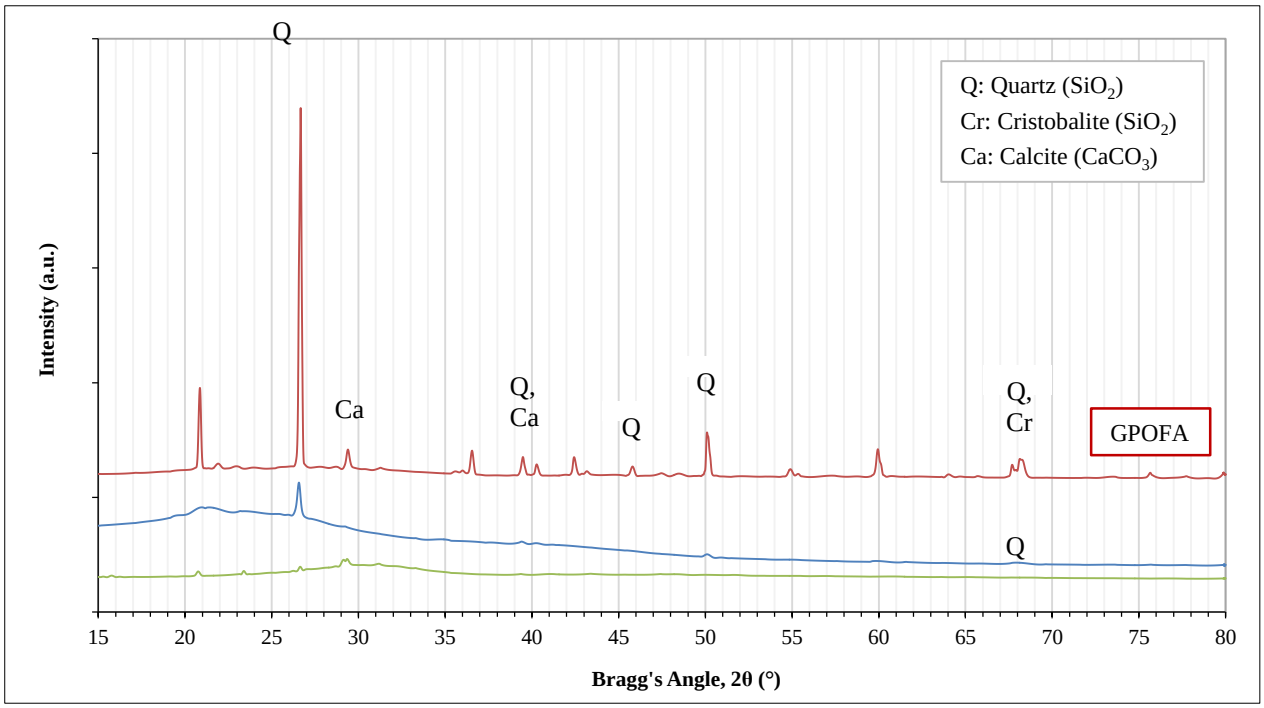

Figure 7. X-Ray Diffractometer of (a) Klias peat, (b) GPOFA, and (c) GGBFS

Meanwhile, Figure 7-b reveals that the GPOFA has detected the presence of three main compounds. The first compound detected was quartz (SiO_2) (ICDD reference: 01-086-1630), with peaks at 2θ = 20.84°, 26.65°, 36.54°, 39.47°, 40.24°, 42.42°, 45.67°, 50.09°, 59.95°, 67.68°, and 68.13°. The highest peak at 2θ = 26.65° shows a substantial content of quartz in its crystalline form, similar to the reports published by Alias Tudin et al. [74]. Furthermore, cristobalite (ICDD reference: 01-076-0941), another form of SiO_2, was also detected, with peaks at 2θ = 21.92°, 42.42°, 59.95°, 67.68°, and 68.12°. The occurrence of quartz and cristobalite reported in this study is consistent with the findings reported by Kroehong et al. [66] and Chandara et al. [75], as cited by Salih et al. [76]. Subsequently, Salih et al. [76] stated that the location of the highest hump was seen from 2θ ranging between 20° and 40°, which indicates an amorphous phase, and this finding was also supported by the results reported by Alias Tudin et al. [74] and Bayer Ozturk and Eren Gultekin [77]. The cristobalite compound is a product of heating the quartz contained in the palm oil waste materials to form raw POFA at high temperatures. Richet et al. [78], as cited by Mysen and Richet [79], stated that the temperature of the quartz-cristobalite transition is at 830°C, and the typical POFA furnace burns at approximately 1000°C [80]. Next, the calcite compound (ICDD reference: 00-005-0586) was also discovered within the GPOFA material, with peaks at 2θ = 29.37° and 39.47°. The presence of calcite can be correlated with the presence of a 12.9% lime (CaO) compound detected in the XRF results.

On the other hand, Figure 7-c presents the mineralogical compound of GGBFS, which did not return any distinctive chemical compounds. However, Figure 7-c showed a characteristic hump at 2θ = 20–30°, which is an indication of the occurrence of quartz in an amorphous phase, and similar findings were reported by [73, 81–83]. The presence of quartz (SiO_2) was also confirmed via the XRF test results, which showed that the GGBFS material contained 27.8% quartz.

4.3. Chemical Composition Characteristics (XRF)

Table 4 shows the breakdown of chemical composition for Klias peat, GPOFA, and GGBFS used in this study in comparison with the findings of other studies. In addition, not only is the XRF test method able to show the major oxides in the sample, but the same XRF data can be further analyzed to show the chemical elements contained within each sample in the similar method done by de Borba et al. [84], Rahgozar & Saberian [85], and Saberian & Rahgozar [86], and the results of the analysis are shown in Table 5.

Table 4. Chemical composition of the geopolymer precursor materials from XRF and LOI tests

Material	SiO_2	Al_2O_3	CaO	Fe_2O_3	K_2O	TiO_2	MgO	SO_3	Others	LOI	Si/Al	Si+Al+Fe
Klias Peat	21.9	10.4	8.4	37.5	1.5	0.7	0	10.5	9.1	3.43	2.11	69.8
Peat [86]	13.7	3.7	26.8	2.9	0.5	0.2	1.6	1.2	49.4	-	3.70	20.3
Raw POFA	48.7	0.9	23.4	5.7	9.4	0.4	4.6	0.5	6.4	1.59	54.11	55.3
GPOFA	62.3	2.3	12.9	3.3	6.8	0.2	6.1	0.3	5.8	0.98	27.09	67.9
GPOFA [27]	45.4	2.1	6.0	2.8	7.1	-	4.8	0.2	31.6	4.96	21.62	50.3
GPOFA [32]	59.8	1.8	10.5	3.2	10.2	0.2	7.2	-	7.1	-	33.2	64.8
GGBFS	27.8	12.8	47.9	0.3	0.3	0.6	5.5	3.6	1.2	2.08	2.17	40.9
GGBFS [31]	34.1	13.5	42.7	0.4	-	-	4.5	-	4.8	1.4	2.53	48.0
GGBFS [11]	31.6	15.3	43.2	0.2	0.5	0.7	6.7	-	1.6	1.4	2.07	47.1

According to the XRF analysis in Table 4, it is found that silicon oxide, aluminum oxide, and iron (III) oxides constitute the major oxides within Klias peat soil. The total of the Si, Al, and Fe oxides for Klias peat amounted to 69.8%, which is an indication that the peat soil itself is a good aluminosilicate source material and fulfills the 50% minimum oxide content required for Class F or Class C pozzolanic compounds [21]. The ratio of Si to Al oxide was valued at 2.11 and is an indication of the good mechanical strength of the compound when the material is activated with alkali, where the recommended Si/Al ratio for geopolymerization is between 2–4 [24]. In a recent work by Saberian & Rahgozar [86], they reported the data on Gavkhuni hemic peat (H_5) obtained from 1.5 m depth from the soil surface, which is obtained at a greater depth compared to the hemic peat studied in this paper. As seen in Table 3, the Gavkhuni hemic peat has a higher amount of silicon oxide and a slightly higher amount of aluminum oxide, but a lower iron (III) oxide content. In addition, the pH value of the Gavkhuni Hemic peat is pH 8.1, which is considered a more alkaline material compared to the pH 3.42 of Klias peat. This is because Klias peat is a tropical peat originating from peat swamp forests and is inherently very acidic [1], while Gavkhuni peat is taken from a fen peatland [86]. Overall, the Si, Al, and Fe oxide total of the Gavkhuni peat (20.9%) is much lower than the sum reported for Klias peat. Despite the same level of decomposition for both peat materials, Huat et al. [1] stated that the chemical composition of peat is dependent on the peat surface altitudes, plant species composition situated near the peatland, the nature of the subsoil, and the peat thickness, which explains the difference between the chemical composition and pH values between both peats.

Table 5. Elements in the Klias peat, raw POFA, GPOFA and GGBFS calculated from XRF data (expressed as percentages of dry mass)

Element	Symbol	Peat	Raw POFA	GPOFA	GGBFS
Aluminum	Al	5.51	0.50	1.23	6.76
Silicon	Si	10.22	22.75	29.11	13.00
Calcium	Ca	5.99	16.71	9.25	34.23
Ferum	Fe	26.21	3.97	2.30	0.24
Oxygen	O	39.91	41.64	45.69	39.56
Magnesium	Mg	-	2.76	3.69	3.32
Manganese	Mn	0.23	0.25	0.16	0.33
Phosphorus	P	2.06	2.21	2.11	0.17
Potassium	K	1.25	7.82	5.66	0.31
Strontium	Sr	0.05	0.23	0.09	0.06
Sulphur	S	4.22	0.22	0.11	1.43
Titanium	Ti	0.40	0.20	0.16	0.35
Zirconium	Zr	0.04	0.06	0.03	0.03
Chloride	Cl	3.06	0.42	0.16	0.13
Lead*	Pb	0.18	-	-	-
Chromium*	Cr	0.10	0.01	0.11	-
Copper*	Cu	0.09	0.10	0.04	-
Zinc*	Zn	0.07	0.04	0.01	-
Nickel*	Ni	0.06	0.01	0.03	-
Arsenic*	As	0.03	-	-	-
Total		**99.36**	**99.88**	**99.84**	**99.93**

* NOTE: Pb, Cr, Cu, Zn, Ni and As are hazardous heavy metals

For POFA material, it can be seen in Table 4 that the mechanical activation (grinding) and oven-drying pre-treatment of raw POFA have managed to change the chemical composition of GPOFA by increasing its silica (SiO_2) content (48.7 to 62.3%) and alumina (Al_2O_3) content (0.9 to 2.3%) but showing a reduction in the lime (CaO) content (23.4 to 12.9%) and hematite (Fe_2O_3) content (5.7 to 3.3%). The substantial amount of lime in raw POFA is attributed to the use of fertilizers in the palm oil estate, as stated by Chindaprasirt et al. [87] and cited by Salih et al. [76]. Subsequently, the chemical composition of GPOFA was found to mainly consist of silica and alumina, with other compounds such as hematite, lime, and periclase (MgO) also observed. According to ASTM C618-19, the GPOFA used in this study has a lime content of 12.9%, which is less than the 18% threshold stipulated in the standard for Class C (high calcium) fly ash [21]. As such, the GPOFA used in this study is classified as Class F and is considered a pozzolan. Ghosh and Ghosh [23] stated that only Class F and Class C pozzolans are considered for geopolymer production in the industry. When compared to the findings of the XRF results published by Asrah et al. [27] and Tonduba et al. [32] for POFA sourced from the same palm oil mill (Lumadan Mill), it can be concluded that the Lumadan POFA used in this study typically has a high silica content ranging from 45–62%, with low amounts of alumina content of 0.9–2.3% and reasonable amounts of lime ranging from 6–23%. The POFA material was classified as Class C pozzolan by Asrah et al. [27] and Tonduba et al. [32] and is different from the classification made by the author's Lumadan POFA classification of Class F pozzolan due to changes made in ASTM C618-19, which saw a revised update to the pozzolan material classification criteria.

The sum of Si, Al, and Fe oxides in Lumadan GPOFA amounts to 67.9%, which also fulfills the 50% oxide requirement outlined in ASTM C618-19. This marks an increase of 12.6% in the total sum of Si, Al, and Fe oxides after grinding. Mashri et al. [88] stated that the increase of these oxides will increase the amount of tobermorite (CSH) formed in the resulting geopolymer mix, which is responsible for the improvement of its mechanical properties. Conversely, the Si/Al ratio of Lumadan GPOFA valued at 27.09 is much higher than the range of 2-4 recommended by Garcia-Lodeiro et al. [24]. This issue will be further discussed in Section 4.5. The POFA characteristics will be analyzed based on a series of criteria, which will determine its suitability as a geopolymer source material.

Subsequently, for the GGBFS material, the main constituents of the material are lime (CaO) and silica (SiO_2), which comprise 75.7% of the total chemical composition. The GGBFS also contains other compounds, such as alumina (Al_2O_3) with 12.8% content and periclase (MgO) at 5.5% content. The presence of 47.9% of lime (CaO) in the GGBFS is significant due to the high concentration of lime, creating a conducive alkaline environment to promote the pozzolanic reaction with the aluminosilicate compounds and contributing to the development of compressive strength and robust

microstructure, as stated by Tsai et al. [89] and cited by Wu et al. [90]. The reaction between GGBFS and the alkali activator solution will produce tobermorite, or Calcium Silicate Hydrate (CSH), and calcite ($CaCO_3$) compounds within the geopolymer matrix [23, 91]. These hydration products, along with the aluminosilicate structure in the slag samples, are expected to contribute to the high strength gain [12].

From Table 5, we can observe that the Klias peat consists mainly of oxygen (O), ferum (Fe), silicon (Si), calcium (Ca), aluminum (Al), and sulphur (S), with the remainder of the elements amounting to 7.92% of the soil mass. According to Garcia-Lodeiro et al. [24], the elements that contribute to the alkaline activated binder reactions from the aluminosilicate materials are Ca, Al, and Si. In the case of Klias peat, the sum of these elements is 21.72% of the dry sample mass, which is relatively high compared to the findings of Andriesse [92]. Moreover, the high percentage of Ca, Si, and Al is imperative to ensure that the peat soil is also a contributor to the geopolymer source material, since these elements are the key to the formation of the cementitious compounds of CASH and NASH compounds through alkali activation [88]. On the other hand, the occurrence of heavy metals in Klias peat, where instances of lead (Pb), chromium (Cr), copper (Cu), zinc (Zn), nickel (Ni), and arsenic (As) were recorded, was similar to the findings reported by Wahab et al. [93]. Previous studies on the presence of heavy metals in Sabah soils were done in limited attempts by Makinda et al. [94] and Soehady Erfen et al. [95]. Further investigation shall be made to ascertain the toxicity levels for these hazardous heavy metals to ensure that the levels comply with local by-laws as specified in MOH Malaysia [96].

Meanwhile, POFA primarily consists of oxygen (O), silicon (Si), calcium (Ca), potassium (K), and ferum (Fe), with the other elements constituting 7.01% (raw POFA) and 7.93% (GPOFA) of the total mass. Mashri et al. [88] stated that the workability and resulting compressive strength of the GPOFA-based geopolymer will be better than those of the raw POFA due to the refined particle size of the GPOFA, which promotes better dissolution of the aluminosilicate material during geopolymerization and improved development of mechanical properties. Furthermore, similar to Klias peat, the POFA materials recorded the presence of chromium, copper, zinc, and nickel elements. An investigation will be carried out on the POFA-based geopolymer compounds to examine the effects of these heavy metals on their compressive strength properties.

Subsequently, for GGBFS, its main constituents are oxygen (O), calcium (Ca), silicon (Si), and aluminum (Al), with the rest of the elements amounting to 6.37% of the sample mass. The GGBFS material was chosen as the second aluminosilicate source to produce geopolymer compounds due to its ability to improve the mechanical and durability properties of fly ash-based geopolymer mixes, as reported by recent studies [11, 82, 97]. This is due to the contribution of the oxygen (O) and calcium (Ca) elements within the GGBFS material, and the GGBFS presence is required in the geopolymer mix in order to maintain the Si/Al ratio of the geopolymer so that it remains between the required range of 2–4, as recommended by Khanday et al. [98]. It is also worth noting that GGBFS does not contain any hazardous heavy metal substances, unlike the Klias peat and Lumadan POFA materials.

4.4. Morphology Characteristics (FESEM Micrographs)

Figures 8-a to 8-d illustrate the FESEM micrographs for Klias peat, GGBFS, pre-treated POFA, and GPOFA used in this research. In Figure 8-a, Klias peat showed the presence of voids, similar to those reported by Sutarno & Mohamad [26], Latifi et al. [99], and Hassan et al. [100], interspersed with particles possessing honeycomb structures, an indication that the peat soil is fibrous [101]. Meanwhile, the GGBFS material seen in Figure 8-b shows particles that are smooth and possess semi-polygonal shapes [102], that are angular [97], and that are sharp-edged in nature [73].

In the case of pre-treated POFA, Figure 8-c shows that it consists of particles with a porous cellular surface, as reported by Khalid et al. [65] and Noorvand et al. [103], which denotes the presence of fibric content [101] and is consistent with the origins of the POFA material produced by burning palm oil waste [29]. Figure 8-c shows that the pre-treated POFA contains clustered spherical particles with minimal voids between these particles, similar to the findings of Lim et al. [67]. Meanwhile, Figure 8-d shows the GPOFA, where upon mechanical activation, the porous cellular surfaces and spherical particles were crushed into particles of smaller sizes, similar to the findings of Salih et al. [76] and Jaturapitakkul et al. [104]. The porous cellular surfaces were seen to have collapsed within the GPOFA due to the grinding action, as reported by Khalid et al. [65].

4.5. Geopolymer Precursor Material Suitability Assessment

Based on the characterization of GPOFA and GGBFS materials made in this section, Ghosh & Ghosh [23] proposed the evaluation of the suitability of both geopolymer precursor materials according to several criteria, as shown in Table 6. For this paper, the listed criteria mainly refer to the ASTM C618-19 [21] standard for the assessment of POFA and the ACI PRC-233-17 Report [22] for the assessment of GGBFS.

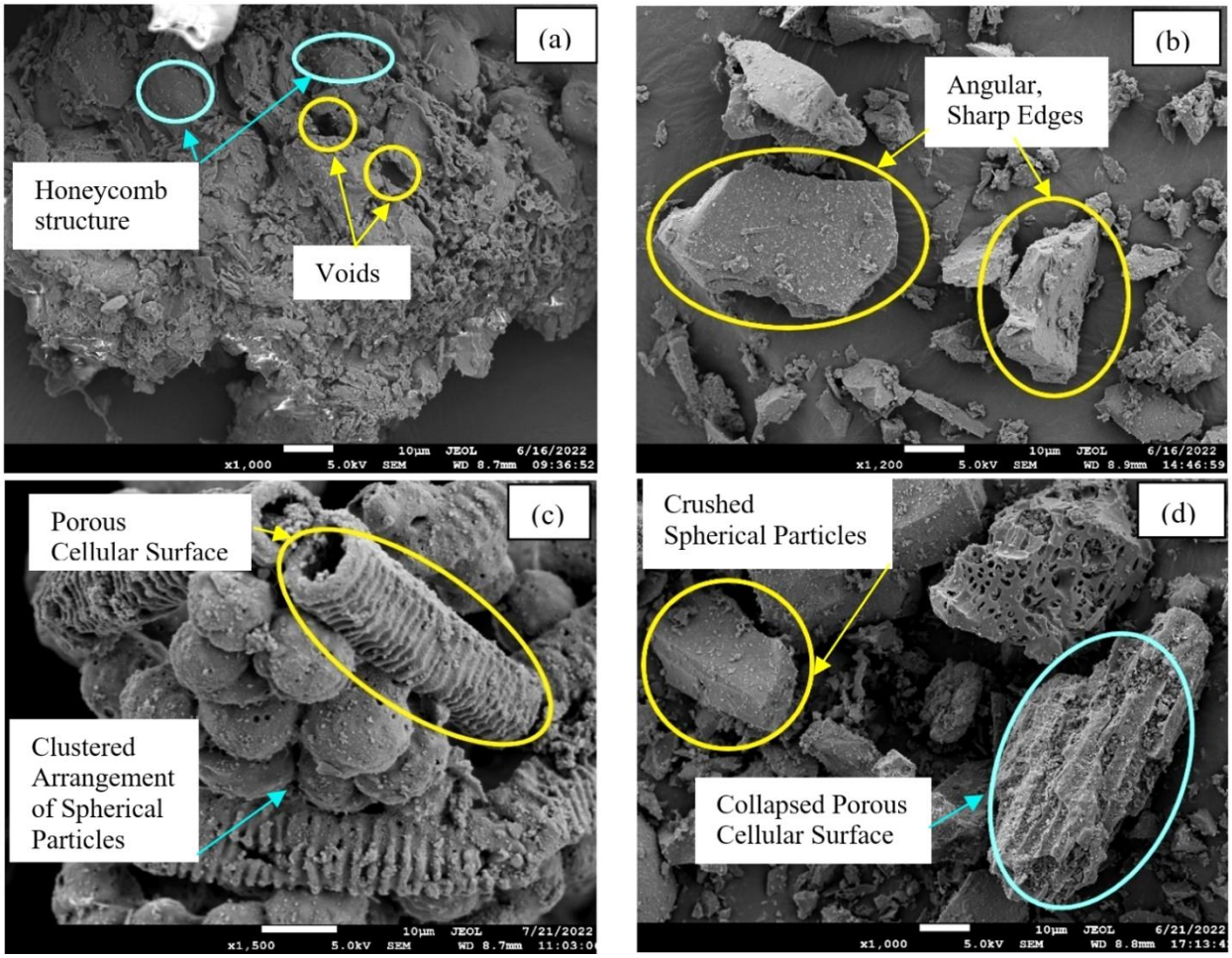

Figure 8. SEM micrographs of (a) Peat, (b) GGBFS, (c) Pre-treated POFA, and (d) GPOFA at 10 µm scale

Table 6. Geopolymer material suitability check for GPOFA and GGBFS

Criteria	Properties of GPOFA	Value	Desired range	Reference	Remarks
1	CaO Content for	12.9	Class F	[21]	Class F
2	SiO_2+Al_2O_3+Fe_2O_3	67.90	Min. 50%	[21]	Acceptable
3	SiO_2	62.30	Min. 40%	[24]	Acceptable
4	SiO_2/Al_2O_3 Ratio	27.09	2 – 4	[23]	Add GGBFS to lower ratio
5	LOI %	0.98	6.0 Max.	[21]	Acceptable
6	Moisture Content	1.87	3.0 Max.	[21]	Acceptable
7	MgO %	6.10	17% Max.	[23]	Acceptable
8	SO_3 %	0.30	5% Max.	[21]	Acceptable
Criteria	Properties of GGBFS	Value	Desired Range	Reference	Remarks
1	CaO/SiO_2 ratio	1.72	0.5 – 2.0	[23]	Acceptable
2	SiO_2/Al_2O_3 ratio	2.17	1.6 – 3.0	[23]	Acceptable
3	Hydration Modulus (HM) = $[(CaO + MgO + Al_2O_3) / SiO_2]$	2.38	Good Hydration HM > 1.4	[25, 105]	Acceptable
4	Basicity Coefficient $K_b = (CaO + MgO)/ (SiO_2 + Al_2O_3)$	1.32	Alkaline (K_b > 1.1)	[106, 107]	Acceptable
5	LOI %	2.08	5% Max.	[23]	Acceptable
6	MgO %	5.5	5 – 15%	[22]	Acceptable
7	SO_3 %	3.6	5% Max.	[22]	Acceptable

For GPOFA, the lime content was valued at 12.9% and is classified as Class F pozzolan, which is the preferred pozzolanic material for geopolymerization [23]. The total Si, Al, and Fe oxides surpassed the minimum 50% limit, valued at 67.9% (as previously reported in Section 4.3). Meanwhile, the silica content of 62.3% is deemed adequate

based on the recommended minimum content of 35%. However, the Si/Al ratio of GPOFA was found to be 27.09, much higher than the recommended value between 2–4 [24]. Furthermore, Davidovits [108], as cited by Ram and Mohanty [109], stated that for materials with a Si/Al ratio between 20 to 35, the aluminosilicate material could be used to produce fire-resistant geopolymer compounds. However, for the current study, the Si/Al ratio will be balanced out to achieve the target ratio of 2-4 by adding GGBFS and alkali activator solutions in the geopolymer mix to produce low-carbon footprint geopolymer compounds with adequate compressive strength. Subsequently, the LOI% was valued at 0.98%, which follows the 6% limit. The moisture content of GPOFA was reported to be 1.87%, which is also below the 3% threshold. Meanwhile, the periclase (MgO) content had a value of 6.1%, which complies with the 17% maximum limit proposed by [23]. The sulphur trioxide (SO_3) content of 0.3% was in line with the requirement of a 5% maximum limit stipulated in [21]. Therefore, the GPOFA material is found to be satisfactory based on seven out of the eight criteria listed in Table 5.

Consequently, in the case of GGBFS, the Lime/Silica ratio was reported to be 1.72, and the Silica/Alumina ratio was valued at 2.17; both ratios were found to be within the desired range recommended by Ghosh & Ghosh [23]. The Hydration Modulus (HM) parameter was introduced by Chang [105], as cited by Manjunath & Narasimhan [25], that quantified the hydration properties for a given material, where the preferred value is 1.4, which indicates good hydration. The GGBFS material has an HM value of 2.38 and is therefore classified as a material with good hydration properties. Another metric to quantify the hydraulic activity of GGBFS is the Basicity Coefficient, K_b, that was proposed by McGannon [110] and was later simplified by Wang et al. [107] and Bakharev et al. [106], which classified a material into three (3) groups, namely: alkaline ($K_b > 1.1$), neutral ($K_b = 0.9–1.1$), and acidic ($K_b < 0.9$). According to Manjunath and Narasimhan [25], neutral and alkaline slags are the ideal source materials for geopolymerization purposes. The GGBFS material used in this study has a K_b value of 1.32 and is classified as an alkaline slag. Subsequently, the LOI registered a value of 2.08%, which is well below the 5% limit. The periclase (MgO) content for GGBFS had a value of 5.5% and is within the range of 5–15% outlined in ACI 233R-17 [22]. Furthermore, the sulphur trioxide (SO_3) content of 3.6% was in line with the requirement of a 5% maximum limit specified in ACI 233R-17 [22].

5. Conclusions

In this study, the physicochemical, chemical composition, mineralogy, and morphology characteristics of Klias peat soil, Lumadan Palm Oil Fuel Ash (POFA), and Ground Granulated Blast Furnace Slag (GGBFS) were established. From the acquired characterization test results, the metal oxides and chemical composition parameters of the aluminosilicate materials (POFA and GGBFS) were used to assess their potential as geopolymer precursor materials. Subsequently, the other parameters established in this characterization study will be used to detect the changes in the physicochemical, chemical composition, mineralogy, and morphology characteristics of the peat, POFA, and GGBFS when all three materials are activated with alkali to create a POFA-GGBFS-soil geopolymer matrix. The findings presented in this paper are part of ongoing research that focuses on the application of alkali-activated POFA-GGBFS blends to improve the shear strength of Klias peat soil. The following conclusions were drawn:

- Based on the results of this study, peat soil, POFA, and GGBFS are found to be suitable materials for the production of geopolymers applied for peat soil stabilization;
- In this paper, Klias peat soil comprises 41.1% coarse grains and 58.9% fine grains, with a mean particle size of 55.48 µm. The natural moisture content and organic content of Klias soil are valued at 657% and 96.57%, respectively. The bulk density of Klias peat was found to be 1.01 g/cm^3, while the specific gravity value was determined to be 1.68. The pH value of 3.02 for the Klias peat is an indication of a highly acidic environment in the peat deposit. Meanwhile, the EC value for Klias peat acquired was 201 µS/cm, and this value is inversely proportional to its organic content. The XRD and XRF tests show that the major component of Klias peat is quartz (SiO_2). FESEM micrographs of Klias peat exhibited the presence of voids with particles possessing honeycomb structures. Therefore, Klias peat can be classified as hemic peat with sufficient aluminosilicate content (Si/Al ratio of 2.11);
- The POFA is identified as a Class F pozzolan. Raw POFA is treated and processed to produce ground POFA with a lower mean particle size in order to promote better geopolymerization. The mean particle size of ground POFA was valued at 17.33 µm, where the material consists of 9.02% coarse grains and 90.98% fine grains. Likewise, the ground POFA moisture content of 1.87% is in compliance with the requirement of ASTM C618-19. The pH value of ground POFA was found to be 8.97, which indicates the highly alkaline nature of the material. Moreover, ground POFA had an EC value of 405 µS/cm that was attributed to lower concentrations of alkali ions and associated hydroxyl ions. In the context of chemical composition, ground POFA contained three main compounds: quartz (SiO_2), cristobalite (SiO_2 in another form), and calcite ($CaCO_3$), which were detected via XRD and XRF tests. The morphology of raw POFA showed the presence of fibric material with a porous cellular surface. With mechanical activation, the raw POFA was crushed into smaller particles, and the cellular surfaces were found to have collapsed as well. Based on the geopolymer suitability criteria, ground POFA is a viable material with adequate Si+Al+Fe oxide content (67.9%), as stipulated by ASTM C618-19;

- The GGBFS material will be used as an enhancer to improve POFA geopolymer production. The GGBFS consists of 95.31% fine grains and 4.69% coarse grains, with the lowest mean particle size of 13.21 µm (in comparison with the peat and POFA materials). Furthermore, the GGBFS has a very low moisture content of 0.93% and is in line with the requirements of ASTM C618-19. The pH value of GGBFS is 8.68, while the EC value was found to be 996 µS/cm. The high EC value is attributed to the significant presence of lime within the material, which was confirmed by the findings from the XRF test showing that the GGBFS chemical composition had 47.9% lime content. Additionally, the material also comprises 27.8% quartz. The micrograph of GGBFS showed that the slag particles are characterized by their semi-polygonal shapes with angular and sharp edges. Based on the geopolymer suitability criteria, GGBFS was found to be suitable for geopolymer production, with a Si/Al ratio of 2.17, a hydration modulus of 2.38 (good hydration), and a Coefficient of 1.32 (alkaline material favorable for geopolymerization);
- According to the geopolymer precursor suitability assessment criteria proposed by Ghosh & Ghosh [23], all the precursor materials were deemed suitable for geopolymerization. Typically, the existing studies on geopolymer materials focus on the metal oxides and chemical composition parameters to assess their suitability as geopolymer source materials. However, the works of Ghosh & Ghosh [23], Garcia-Lodeiro et al., and Manjunath and Narasimhan [25] were incorporated to improve the material suitability criteria, which include new parameters such as hydration modulus and basicity coefficient. Subsequently, the authors found that this study is the first attempt at assessing POFA as a viable geopolymer source material based on the requirements listed in Table 6, Section 4.5. Therefore, it is hoped that the example of suitability assessment carried out in Section 4.5 serves as a reference for future research works pertaining to geopolymer material studies. Furthermore, the authors believe that the desired ranges for the 15 criteria proposed in Table 6 can be improved further with the inclusion of more datasets published by other researchers with a wider range of physical and chemical characteristics of the precursor materials derived from other industrial and agricultural wastes, since the current assessment criteria is based on fly ash, raw or calcined natural pozzolans, and blast furnace slag materials only;
- Based on the results of this study, planned works involving the testing program on the geopolymerization of POFA-GGBFS-peat soil blends at ambient temperature will be carried out in the near future. As stated in a recent review carried out by the author, a thorough experimental investigation should be carried out to examine the effectiveness of POFA-GGBFS geopolymer as a soil stabilizer material for Klias peat. The optimal use of alkali-activated POFA-GGBFS blends to produce geopolymers results in an effective way to manage agricultural and industrial wastes, which promotes sustainable development solutions for the construction industry [5].

6. Declarations

6.1. Author Contributions

Conceptualization, A.E.A., H.A., and H.M.M.; methodology: A.E.A., H.Z.A., and N.A.A.; formal analysis: A.E.A., H.Z.A., and N.A.A.; resources, A.E.A, H.A., and H.M.M.; writing—original draft preparation, A.E.A.; writing—review and editing, A.E.A., H.A., H.M.M., H.Z.A., and N.A.A.; visualization, A.E.A. and H.A.; supervision, H.A. and H.M.M.; project administration, A.E.A. and H.A.; funding acquisition, H.A. and H.M.M. All authors have read and agreed to the published version of the manuscript.

6.2. Data Availability Statement

The data presented in this study are available on request from the corresponding author.

6.3. Funding and Acknowledgements

The first author is thankful to the Ministry of Higher Education, Malaysia, for the Ph.D. Scholarship. The authors acknowledge the funding support from the Centre for Research and Innovation, Universiti Malaysia Sabah (UMS) for this research project and publication, under the UMSGreat Grant (GUG0566-1/2022). This work is also supported by the Faculty of Engineering (FKJ) and Centre For Instrumentation and Science Services (CFISS), UMS, which provided the facilities required to carry out the planned research works. The authors acknowledge the support of Sawit Kinabalu Pvt. Ltd. for providing the Palm Oil Fuel Ash material used in this research.

6.4. Institutional Review Board Statement

Not applicable.

6.5. Informed Consent Statement

Not applicable.

6.6. Declaration of Competing Interest

The authors declare that they have no known competing financial interests or personal relationships that could have appeared to influence the work reported in this paper.

7. References

[1] Huat, B. B., Prasad, A., Asadi, A., & Kazemian, S. (2014). Geotechnics of organic soils and peat. CRC Press, London, United Kingdom. doi:10.1201/b15627.

[2] Rikmann, E., Zekker, I., Teppand, T., Pallav, V., Shanskiy, M., Mäeorg, U., Tenno, T., Burlakovs, J., & Liiv, J. (2021). Relationship between phase composition and mechanical properties of peat soils stabilized using oil shale ash and pozzolanic additive. Water (Switzerland), 13(7), 942. doi:10.3390/w13070942.

[3] Nicholson, P. G. (2015). Soil improvement and ground modification methods. Butterworth-Heinemann, Oxford, United Kingdom. doi:10.1016/C2012-0-02804-9.

[4] Noor Azline, M. N., Abd Aziz, F. N. A., & Suleiman Juma, A. (2015). Effect of Ground Granulated Blast Furnace Slag on Compressive Strength of POFA Blended Concrete. Applied Mechanics and Materials, 802, 142–148. doi:10.4028/www.scientific.net/amm.802.142.

[5] Qaidi, S., Najm, H. M., Abed, S. M., Ahmed, H. U., Al Dughaishi, H., Al Lawati, J., Sabri, M. M., Alkhatib, F., & Milad, A. (2022). Fly Ash-Based Geopolymer Composites: A Review of the Compressive Strength and Microstructure Analysis. Materials, 15(20), 7098. doi:10.3390/ma15207098.

[6] Adhikari, B., Khattak, M. J., & Adhikari, S. (2021). Mechanical and durability characteristics of flyash-based soil-geopolymer mixtures for pavement base and subbase layers. International Journal of Pavement Engineering, 22(9), 1193–1212. doi:10.1080/10298436.2019.1668562.

[7] Khasib, I. A., & Daud, N. N. N. (2020). Physical and Mechanical Study of Palm Oil Fuel Ash (POFA) based Geopolymer as a Stabilizer for Soft Soil. Applied Engineering and Sciences, 28(S2). doi:10.47836/pjst.28.s2.12.

[8] Arulrajah, A., Kua, T.-A., Phetchuay, C., Horpibulsuk, S., Mahghoolpilehrood, F., & Disfani, M. M. (2016). Spent Coffee Grounds–Fly Ash Geopolymer Used as an Embankment Structural Fill Material. Journal of Materials in Civil Engineering, 28(5), 4015197. doi:10.1061/(asce)mt.1943-5533.0001496.

[9] Chung, L. L. P., Wong, Y. C., & Arulrajah, A. (2021). The Application of Spent Coffee Grounds and Tea Wastes as Additives in Alkali-Activated Bricks. Waste and Biomass Valorization, 12(11), 6273–6291. doi:10.1007/s12649-021-01453-7.

[10] Cristelo, N., Glendinning, S., Fernandes, L., & Pinto, A. T. (2013). Effects of alkaline-activated fly ash and Portland cement on soft soil stabilisation. Acta Geotechnica, 8(4), 395–405. doi:10.1007/s11440-012-0200-9.

[11] Chen, K., Wu, D., Zhang, Z., Pan, C., Shen, X., Xia, L., & Zang, J. (2022). Modeling and optimization of fly ash–slag-based geopolymer using response surface method and its application in soft soil stabilization. Construction and Building Materials, 315, 125723. doi:10.1016/j.conbuildmat.2021.125723.

[12] Khanday, S. A., Hussain, M., & Das, A. K. (2021). Stabilization of Indian peat using alkali-activated ground granulated blast furnace slag. Bulletin of Engineering Geology and the Environment, 80(7), 5539–5551. doi:10.1007/s10064-021-02248-9.

[13] Abdeldjouad, L., Asadi, A., Nahazanan, H., Huat, B. B. K., Dheyab, W., & Elkhebu, A. G. (2019). Effect of Clay Content on Soil Stabilization with Alkaline Activation. International Journal of Geosynthetics and Ground Engineering, 5, 4. doi:10.1007/s40891-019-0157-y.

[14] Khasib, I. A., Daud, N. N. N., & Nasir, N. A. M. (2021). Strength development and microstructural behavior of soils stabilized with palm oil fuel ash (POFA)-based geopolymer. Applied Sciences (Switzerland), 11(8), 3572. doi:10.3390/app11083572.

[15] Zainuddin, A. N., Mukri, M., & Sidek, N. (2022). Investigation on Soil Strength and Microstructure of Palm Oil Boiler Ash with Sodium Hydroxide and Sodium Silicate as Alkaline Solution. International Journal of Sustainable Construction Engineering and Technology, 13(1), 57–67. doi:10.30880/ijscet.2022.13.01.006.

[16] Yahya, Z., Abdullah, M. M. A. B., Hussin, K., Ismail, K. N., Razak, R. A., & Sandu, A. V. (2015). Effect of solids-to-liquids, Na2SiO3-to-NaOH and curing temperature on the palm oil boiler ash (Si + Ca) geopolymerisation system. Materials, 8(5), 2227–2242. doi:10.3390/ma8052227.

[17] Kwek, S. Y., Awang, H., & Cheah, C. B. (2021). Influence of liquid-to-solid and alkaline activator (Sodium silicate to sodium hydroxide) ratios on fresh and hardened properties of alkali-activated palm oil fuel ash geopolymer. Materials, 14(15), 4253. doi:10.3390/ma14154253.

[18] Amaludin, A. E., Asrah, H., & Mohamad, H. M. (2023). A Review of Advances in Peat Soil Stabilisation Technology: Exploring the Potential of Palm Oil Fuel Ash Geopolymer as a Soil Stabiliser Material. Civil Engineering Journal (Iran), 9(8), 2085–2104. doi:10.28991/CEJ-2023-09-08-017.

[19] Abdullah, H. H. (2020). An experimental investigation on stabilisation of clay soils with fly-ash based geopolymer. Ph.D. Thesis, Curtin University, Perth, Australia.

[20] Pourakbar, S., Asadi, A., Huat, B. B. K., & Fasihnikoutalab, M. H. (2015). Soil stabilisation with alkali-activated agro-waste. Environmental Geotechnics, 2(6), 359–370. doi:10.1680/envgeo.15.00009.

[21] ASTM C618. (2010). Standard Specification for Coal Fly Ash and Raw or Calcined Natural Pozzolan for Use in Concrete. ASTM International, Pennsylvania, United States. doi:10.1520/C0618-19.2.

[22] ACI 233R-17. (2017). Guide to the Use of Slag Cement in Concrete and Mortar. American Concrete Institute (ACI), Michigan, United States.

[23] Ghosh, K., & Ghosh, P. (2020). Alkali Activated Fly Ash: Blast Furnace Slag Composites. CRC Press, Boca Raton, United States. doi:10.1201/9781003082460.

[24] Garcia-Lodeiro, I., Palomo, A., & Fernández-Jiménez, A. (2015). An overview of the chemistry of alkali-activated cement-based binders. Handbook of alkali-activated cements, mortars and concretes, 19-47, Woodhead Publishing, Sawston, United Kingdom. doi:10.1533/9781782422884.1.19.

[25] Manjunath, R., & Narasimhan, M. C. (2020). Alkali-activated concrete systems: a state of art. New Materials in Civil Engineering, 459–491, Butterworth-Heinemann, Oxford, United Kingdom. doi:10.1016/b978-0-12-818961-0.00013-2.

[26] Mohamad, H. M., Zainorabidin, A., & Mohamad, M. I. (2022). Maximum Strain Effect and Secant Modulus Variation of Hemic Peat Soil at large Deformation due to Cyclic Loading. Civil Engineering Journal, 8(10), 2243-2260. doi:10.28991/CEJ-2022-08-10-015.

[27] Asrah, H., Mirasa, A. K., & Mannan, A. (2015). The performance of ultrafine palm oil fuel ash in suppressing the alkali silica reaction in mortar bar. International Journal of Engineering Applied Science, 9, 60-66.

[28] Tonduba, Y. W., Mirasa, A. K., & Asrah, H. (2021). Utilization of Ultrafine Palm Oil Fuel Ash in Interlocking Compressed Earth Brick. International Journal of GEOMATE, 21(87), 70–78. doi:10.21660/2021.87.j2245.

[29] Hamada, H. M., Thomas, B. S., Yahaya, F. M., Muthusamy, K., Yang, J., Abdalla, J. A., & Hawileh, R. A. (2021). Sustainable use of palm oil fuel ash as a supplementary cementitious material: A comprehensive review. Journal of Building Engineering, 40, 102286. doi:10.1016/j.jobe.2021.102286.

[30] Islam, A., Alengaram, U. J., Jumaat, M. Z., & Bashar, I. I. (2014). The development of compressive strength of ground granulated blast furnace slag-palm oil fuel ash-fly ash based geopolymer mortar. Materials Design (1980-2015), 56, 833–841. doi:10.1016/j.matdes.2013.11.080.

[31] Salih, M. A., Farzadnia, N., Abang Ali, A. A., & Demirboga, R. (2015). Development of high strength alkali activated binder using palm oil fuel ash and GGBS at ambient temperature. Construction and Building Materials, 93, 289–300. doi:10.1016/j.conbuildmat.2015.05.119.

[32] Tonduba, Y. W., Mirasa, A. K., & Asrah, H. (2019). Applicability of Palm Oil Fuel Ash in Interlocking Compressed Earth Brick - A Preliminary Assessment. Journal of Physics: Conference Series, 1358(1), 12027. doi:10.1088/1742-6596/1358/1/012027.

[33] Sas, W., Dzięcioł, J., Radzevičius, A., Radziemska, M., Dapkienė, M., Šadzevičius, R., Skominas, R., & Głuchowski, A. (2021). Geotechnical and Environmental Assessment of Blast Furnace Slag for Engineering Applications. Materials, 14(20), 6029. doi:10.3390/ma14206029.

[34] Abdila, S. R., Abdullah, M. M. A. B., Ahmad, R., Nergis, D. D. B., Rahim, S. Z. A., Omar, M. F., Sandu, A. V., Vizureanu, P., & Syafwandi. (2022). Potential of Soil Stabilization Using Ground Granulated Blast Furnace Slag (GGBFS) and Fly Ash via Geopolymerization Method: A Review. Materials, 15(1), 375. doi:10.3390/ma15010375.

[35] ISO 13320. (2020). Particle Size Analysis-Laser Diffraction Methods. International Organization for Standardization (ISO), Vernier, Geneva, Switzerland.

[36] Arvaniti, E. C., Juenger, M. C. G., Bernal, S. A., Duchesne, J., Courard, L., Leroy, S., Provis, J. L., Klemm, A., & De Belie, N. (2015). Physical characterization methods for supplementary cementitious materials. Materials and Structures/Materiaux et Constructions, 48(11), 3675–3686. doi:10.1617/s11527-014-0430-4.

[37] Cyr, M., & Tagnit-Hamou, A. (2001). Particle size distribution of fine powders by LASER diffraction spectrometry. Case of cementitious materials. Materials and Structures/Materiaux et Constructions, 34(6), 342–350. doi:10.1007/bf02486485.

[38] Polakowski, C., Ryżak, M., Sochan, A., Beczek, M., Mazur, R., & Bieganowski, A. (2021). Particle size distribution of various soil materials measured by laser diffraction—the problem of reproducibility. Minerals, 11(5). doi:10.3390/min11050465.

[39] Jewell, R., & Rathbone, R. (2009). Optical Properties of Coal Combustion Byproducts for Particle-Size Analysis by Laser Diffraction. Coal Combustion and Gasification Products, 1(1), 1–6. doi:10.4177/ccgp-d-09-00001.

[40] von Post, L. (1922). Sweden's Geological Survey's peat inventory and some of its results so far. Swedish Moss Culture Association's Journal. (In Swedish)

[41] BS 1377-2: 1990 (1990). Methods of Test for Soil for Civil Engineering Purposes – Part 2: Classification tests. British Standard, London, United Kingdom.

[42] BS 1377-3: 1990 (1990). Methods of Test for Soil for Civil Engineering Purposes – Part 3: Chemical and electro-chemical tests. British Standard, London, United Kingdom.

[43] O'Kelly, B. C. (2022). Discussion of "Physio-Chemical Properties, Consolidation, and Stabilization of Tropical Peat Soil Using Traditional Soil Additives — A State of the Art Literature Review" by Afnan Ahmada, Muslich Hartadi Sutantoa, Mohammed Ali Mohammed Al-Bareda, Indra Sati Hamonangan Harahapa, Seyed Vahid Alavi Nezhad Khalil Abada, Mudassir Ali Khana. KSCE Journal of Civil Engineering, 26(8), 3455–3459. doi:10.1007/s12205-022-2313-5.

[44] Mironova, N., Yefremova, O., Biletska, H., Bloshchynskyi, I., Koshelnyk, I., Sych, S., ... & Kravchuk, V. (2022). Soil quality evaluation in urban ecosystems during the covid-19 pandemic. HighTech and Innovation Journal, 3, 43-51. doi:10.28991/HIJ-SP2022-03-04.

[45] BS 1377-9: 1990 (1990). Methods of Test for Soil for Civil Engineering Purposes – Part 9: In Situ tests. British Standard, London, United Kingdom.

[46] ASTM D2976-22. (2022). Standard Test Method for pH of Peat Materials. ASTM International, Pennsylvania, United States. doi:10.1520/D2976-22.

[47] Rauch, A. F., Katz, L. E., & Liljestrand, H. M. (1993). Aa analysis of the mechanisms and efficacy of three liquid chemical soil stabilizers. FHWA/TX-03/1993-1, Volume 1, University of Texas, Austin, United States.

[48] Kumar, D., Soni, A., & Kumar, M. (2022). Retrieval of Land Surface Temperature from Landsat-8 Thermal Infrared Sensor Data. Journal of Human, Earth, and Future, 3(2), 159-168. doi:10.28991/HEF-2022-03-02-02.

[49] Khan, H., Yerramilli, A. S., D'Oliveira, A., Alford, T. L., Boffito, D. C., & Patience, G. S. (2020). Experimental methods in chemical engineering: X-ray diffraction spectroscopy—XRD. Canadian Journal of Chemical Engineering, 98(6), 1255–1266. doi:10.1002/cjce.23747.

[50] Gates-Rector, S., & Blanton, T. (2019). The Powder Diffraction File: a quality materials characterization database. Powder Diffraction, 34(4), 352–360. doi:10.1017/S0885715619000812.

[51] Yusuf, T. O. (2015). Effects of palm oil fuel ash and metakaolin blend on properties of geopolymer mortar. PhD Thesis, Universiti Teknologi Malaysia, Skudai, Malaysia.

[52] ASTM E1621-21. (2021). Standard Guide for Elemental Analysis by Wavelength Dispersive X-Ray Fluorescence Spectrometry. ASTM International, Pennsylvania, United States. doi:10.1520/E1621-21.

[53] Khadayeir, A. A., Wannas, A. H., & Yousif, F. H. (2022). Effect of Applying Cold Plasma on Structural, Antibacterial and Self Cleaning Properties of α-Fe2O3 (HEMATITE) Thin Film. Emerging Science Journal, 6(1), 75-85. doi:10.28991/ESJ-2022-06-01-06.

[54] Khare, T., Oak, U., Shriram, V., Verma, S. K., & Kumar, V. (2019). Biologically synthesized nanomaterials and their antimicrobial potentials. Comprehensive Analytical Chemistry, 263–289, Elsevier, Amsterdam, Netherlands. doi:10.1016/bs.coac.2019.09.002.

[55] ASTM E986-04. (2017). Standard Practice for Scanning Electron Microscope Beam Size Characterization. ASTM International, Pennsylvania, United States. doi:10.1520/E0986-04R17.

[56] Huggett, J. M., & Shaw, H. F. (1997). Field emission scanning electron microscopy — a high-resolution technique for the study of clay minerals in sediments. Clay Minerals, 32(2), 197–203. doi:10.1180/claymin.1997.032.2.03.

[57] Nguyen, J. N. T., & Harbison, A. M. (2017). Scanning Electron Microscopy Sample Preparation and Imaging. Molecular Profiling, 71–84, Springer. doi:10.1007/978-1-4939-6990-6_5.

[58] Mohamad, H. M., Zainorabidin, A., Musta, B., Mustafa, M. N., Amaludin, A. E., & Abdurahman, M. N. (2021). Compressibility behaviour and engineering properties of north Borneo peat soil. Eurasian Journal of Soil Science, 10(3), 259–268. doi:10.18393/ejss.930620.

[59] Sapar, N. I. F., Matlan, S. J., Mohamad, H. M., Alias, R., & Ibrahim, A. (2020). a Study on Physical and Morphological Characteristics of. International Journal of Advanced Research, in Engineering and Technology, 11(11), 542–553. doi:10.34218/IJARET.11.11.2020.051.

[60] Paul, A., & Hussain, M. (2020). Sustainable Use of GGBS and RHA as a Partial Replacement of Cement in the Stabilization of Indian Peat. International Journal of Geosynthetics and Ground Engineering, 6, 4. doi:10.1007/s40891-020-0185-7.

[61] Paul, A., & Hussain, M. (2020). Cement Stabilization of Indian Peat: An Experimental Investigation. Journal of Materials in Civil Engineering, 32(11), 4020350. doi:10.1061/(asce)mt.1943-5533.0003363.

[62] Lau, J., Biscontin, G., & Berti, D. (2023). Effects of biochar on cement-stabilised peat soil. Proceedings of the Institution of Civil Engineers: Ground Improvement, 176(2), 76–87. doi:10.1680/jgrim.19.00013.

[63] Tremblay, H., Duchesne, J., Locat, J., & Leroueil, S. (2002). Influence of the nature of organic compounds on fine soil stabilization with cement. Canadian Geotechnical Journal, 39(3), 535–546. doi:10.1139/t02-002.

[64] Paul, A., & Hussain, M. (2022). pH and Electrical Conductivity of Cement-Treated Peat. Proceedings of the 7th Indian Young Geotechnical Engineers Conference, 167–173, Springer, Singapore. doi:10.1007/978-981-16-6456-4_19.

[65] Khalid, N. H. A., Hussin, M. W., Mirza, J., Ariffin, N. F., Ismail, M. A., Lee, H.-S., Mohamed, A., & Jaya, R. P. (2016). Palm oil fuel ash as potential green micro-filler in polymer concrete. Construction and Building Materials, 102, 950–960. doi:10.1016/j.conbuildmat.2015.11.038.

[66] Kroehong, W., Sinsiri, T., Jaturapitakkul, C., & Chindaprasirt, P. (2011). Effect of palm oil fuel ash fineness on the microstructure of blended cement paste. Construction and Building Materials, 25(11), 4095–4104. doi:10.1016/j.conbuildmat.2011.04.062.

[67] Lim, N. H. A. S., Ismail, M. A., Lee, H. S., Hussin, M. W., Sam, A. R. M., & Samadi, M. (2015). The effects of high volume nano palm oil fuel ash on microstructure properties and hydration temperature of mortar. Construction and Building Materials, 93, 29–34. doi:10.1016/j.conbuildmat.2015.05.107.

[68] Lim, A., Mirasa, A. K., Asrah, H., & Tian, X. (2022). Maximizing Volume of Spent Bleaching Earth Ash (Sbea) Pozzolan Used As Cement Replacement in Mortar Through Mechanical Activation. Jurnal Teknologi/Technology Journal, 84(5), 105–116. doi:10.11113/jurnalteknologi.v84.18177.

[69] ASTM C989-09. (2009). Standard Specification for Slag Cement for Use in Concrete and Mortars. ASTM International, Pennsylvania, United States.

[70] Chesner, W. H., Collins, R. J., MacKay, M. H., & Emery, J. (2002). User guidelines for waste and by-product materials in pavement construction. FHWA-RD-97-148, Guideline Manual, Report No. 480017. Recycled Materials Resource Center, Federal Highway Administration, Washington, United States.

[71] Shehata, M. H., Thomas, M. D. A., & Bleszynski, R. F. (1999). The effects of fly ash composition on the chemistry of pore solution in hydrated cement pastes. Cement and Concrete Research, 29(12), 1915–1920. doi:10.1016/S0008-8846(99)00190-8.

[72] Dinakar, P., Kartik Reddy, M., & Sharma, M. (2013). Behaviour of self-compacting concrete using Portland pozzolana cement with different levels of fly ash. Materials and Design, 46, 609–616. doi:10.1016/j.matdes.2012.11.015.

[73] Abdila, S. R., Abdullah, M. M. A. B., Ahmad, R., Rahim, S. Z. A., Rychta, M., Wnuk, I., Nabiałek, M., Muskalski, K., Tahir, M. F. M., Syafwandi, Isradi, M., & Gucwa, M. (2021). Evaluation on the mechanical properties of ground granulated blast slag (GGBS) and fly ash stabilized soil via geopolymer process. Materials, 14(11), 1–19. doi:10.3390/ma14112833.

[74] Alias Tudin, D. Z., Rizalman, A. N., & Asrah, H. (2018). Performance of Palm Oil Fuel Ash and Rice Husk Ash Based Geopolymer Mortar. E3S Web of Conferences, 65, 02011. doi:10.1051/e3sconf/20186502011.

[75] Chandara, C., Sakai, E., Azizli, K. A. M., Ahmad, Z. A., & Hashim, S. F. S. (2010). The effect of unburned carbon in palm oil fuel ash on fluidity of cement pastes containing superplasticizer. Construction and Building Materials, 24(9), 1590–1593. doi:10.1016/j.conbuildmat.2010.02.036.

[76] Salih, M. A., Abang Ali, A. A., & Farzadnia, N. (2014). Characterization of mechanical and microstructural properties of palm oil fuel ash geopolymer cement paste. Construction and Building Materials, 65, 592–603. doi:10.1016/j.conbuildmat.2014.05.031.

[77] Bayer Ozturk, Z., & Eren Gultekin, E. (2015). Preparation of ceramic wall tiling derived from blast furnace slag. Ceramics International, 41(9), 12020–12026. doi:10.1016/j.ceramint.2015.06.014.

[78] Richet, P., Bottinga, Y., Denielou, L., Petitet, J. P., & Tequi, C. (1982). Thermodynamic properties of quartz, cristobalite and amorphous SiO2: drop calorimetry measurements between 1000 and 1800 K and a review from 0 to 2000 K. Geochimica et Cosmochimica Acta, 46(12), 2639–2658. doi:10.1016/0016-7037(82)90383-0.

[79] Mysen, B., & Richet, P. (2019). Silica. Silicate Glasses and Melts, 143–183, Elsevier Science, Amsterdam, Netherlands. doi:10.1016/b978-0-444-63708-6.00005-3.

[80] Amran, M., Murali, G., Fediuk, R., Vatin, N., Vasilev, Y., & Abdelgader, H. (2021). Palm oil fuel ash-based eco-efficient concrete: A critical review of the short-term properties. Materials, 14(2), 1–33. doi:10.3390/ma14020332.

[81] Türker, H. T., Balçikanli, M., Durmuş, I. H., Özbay, E., & Erdemir, M. (2016). Microstructural alteration of alkali activated slag mortars depend on exposed high temperature level. Construction and Building Materials, 104, 169–180. doi:10.1016/j.conbuildmat.2015.12.070.

[82] Bellum, R. R., Muniraj, K., & Madduru, S. R. C. (2020). Influence of slag on mechanical and durability properties of fly ash-based geopolymer concrete. Journal of the Korean Ceramic Society, 57(5), 530–545. doi:10.1007/s43207-020-00056-7.

[83] Abd Rahman, R. F., Asrah, H., Rizalman, A. N., Mirasa, A. K., & Rajak, M. A. A. (2020). 'Study of Eco-Processed Pozzolan Characterization as Partial Replacement of Cement. Journal of Environmental Treatment Techniques, 8(3), 967-970.

[84] de Borba, W. F., Silvério da Silva, J. L., da Cunha Kemerich, P. D., Boito de Souza, É. E., D'ávila Fernandes, G., & Carvalho, I. R. (2020). Analysis of Chemical Features of a Soil Used as Landfill: Using the X-Ray Fluorescence (XRF) Technique. Water, Air, and Soil Pollution, 231(6), 231. doi:10.1007/s11270-020-04668-x.

[85] Rahgozar, M. A., and Saberian, M. (2015). Physical and Chemical Properties of two Iranian Peat Types. Mires and Peat, 16 (07), 1–17.

[86] Saberian, M., & Rahgozar, M. A. (2016). Geotechnical properties of peat soil stabilised with shredded waste tyre chips in combination with gypsum, lime or cement. Mires and Peat, 18, 1–16. doi:10.19189/MaP.2015.OMB.211.

[87] Chindaprasirt, P., Rukzon, S., & Sirivivatnanon, V. (2008). Resistance to chloride penetration of blended Portland cement mortar containing palm oil fuel ash, rice husk ash and fly ash. Construction and Building Materials, 22(5), 932–938. doi:10.1016/j.conbuildmat.2006.12.001.

[88] Mashri, M. O. M., Megat Johari, M. A., Ahmad, Z. A., & Mijarsh, M. J. A. (2022). Influence of milling process of palm oil fuel ash on the properties of palm oil fuel ash-based alkali activated mortar. Case Studies in Construction Materials, 16, 857. doi:10.1016/j.cscm.2021.e00857.

[89] Tsai, C. J., Huang, R., Lin, W. T., & Wang, H. N. (2014). Mechanical and cementitious characteristics of ground granulated blast furnace slag and basic oxygen furnace slag blended mortar. Materials and Design, 60, 267–273. doi:10.1016/j.matdes.2014.04.002.

[90] Wu, Y. H., Huang, R., Tsai, C. J., & Lin, W. T. (2015). Recycling of sustainable co-firing fly ashes as an alkali activator for GGBS in blended cements. Materials, 8(2), 784–798. doi:10.3390/ma8020784.

[91] Abdullah, H. H., & Shahin, M. A. (2019). Strength Characteristics of Clay Stabilized with Fly-ash Based Geopolymer Incorporating Granulated Slag. Proceedings of the 4th World Congress on Civil, Structural, and Environmental Engineering. doi:10.11159/icgre19.139.

[92] Andriesse, J. P. (1988). Nature and management of tropical peat soils (No. 59). Food & Agriculture Organization, Rome, Italy.

[93] Wahab, A., Hassan, M., Din, Z. U., & Zaman, Q. U. (2021). Heavy metals concentration in undisturbed peat soil at Pekan District, Pahang, West Malaysia. Maejo International Journal of Energy and Environmental Communication, 3(2), 23-31. doi:10.54279/mijeec.v3i2.245731.

[94] Makinda, J., Kassim K. A., Siong, C. C., Zango, M. U., & Muhammed, A. S. (2020). Geochemical Evaluation of Contaminated Soil for Stabilisation using Microbiologically Induced Calcite Precipitation Method. International Journal of Advanced Science and Technology, 29, 2375–2382.

[95] Soehady Erfen, H. F. W., Asis, J., Abdullah, M., Musta, B., Tahir, S., Pungut, H., & Mohd Husin, M. A. Y. (2017). Geochemical Characterization of Sediments around Nukakatan Valley, Tambunan, Sabah. Geological Behavior, 1(1), 13–15. doi:10.26480/gbr.01.2017.13.15.

[96] MOH Malaysia. (2016). National Standard for Drinking Water Quality. Engineering Services Division Ministry of Health Malaysia. Available online: https://faolex.fao.org/docs/pdf/mal189903.pdf (accessed on April 2023).

[97] Wu, D., Zhang, Z., Chen, K., & Xia, L. (2022). Experimental Investigation and Mechanism of Fly Ash/Slag-Based Geopolymer-Stabilized Soft Soil. Applied Sciences (Switzerland), 12(15), 7438. doi:10.3390/app12157438.

[98] Khanday, S. A., Hussain, M., & Das, A. K. (2021). Rice Husk Ash–Based Geopolymer Stabilization of Indian Peat: Experimental Investigation. Journal of Materials in Civil Engineering, 33(12), 4021347. doi:10.1061/(asce)mt.1943-5533.0003982.

[99] Latifi, N., Siddiqua, S., & Marto, A. (2019). Stabilization of tropical peat using liquid polymer. Environmental Science and Engineering, 2, 826–833. doi:10.1007/978-981-13-2221-1_94.

[100] Hassan, W. H. W., Rashid, A. S. A., Latifi, N., Horpibulsuk, S., & Borhamdin, S. (2017). Strength and morphological characteristics of organic soil stabilized with magnesium chloride. Quarterly Journal of Engineering Geology and Hydrogeology, 50(4), 454–459. doi:10.1144/qjegh2016-124.

[101] Ahmad Afip, I., Taib, S. N. L., Jusoff, K., & Afip, L. A. (2019). Measurement of Peat Soil Shear Strength Using Wenner Four-Point Probes and Vane Shear Strength Methods. International Journal of Geophysics, 2019, 1–12. doi:10.1155/2019/3909032.

[102] Arulrajah, A., Yaghoubi, M., Disfani, M. M., Horpibulsuk, S., Bo, M. W., & Leong, M. (2018). Evaluation of fly ash- and slag-based geopolymers for the improvement of a soft marine clay by deep soil mixing. Soils and Foundations, 58(6), 1358–1370. doi:10.1016/j.sandf.2018.07.005.

[103] Noorvand, H., Ali, A. A. A., Demirboga, R., Noorvand, H., & Farzadnia, N. (2013). Physical and chemical characteristics of unground palm oil fuel ash cement mortars with nanosilica. Construction and Building Materials, 48, 1104–1113. doi:10.1016/j.conbuildmat.2013.07.070.

[104] Jaturapitakkul, C., Tangpagasit, J., Songmue, S., & Kiattikomol, K. (2011). Filler effect and pozzolanic reaction of ground palm oil fuel ash. Construction and Building Materials, 25(11), 4287–4293. doi:10.1016/j.conbuildmat.2011.04.073.

[105] Chang, J. J. (2003). A study on the setting characteristics of sodium silicate-activated slag pastes. Cement and Concrete Research, 33(7), 1005–1011. doi:10.1016/S0008-8846(02)01096-7.

[106] Bakharev, T., Sanjayan, J. G., & Cheng, Y. B. (2000). Effect of admixtures on properties of alkali-activated slag concrete. Cement and Concrete Research, 30(9), 1367–1374. doi:10.1016/S0008-8846(00)00349-5.

[107] Wang, S. D., Scrivener, K. L., & Pratt, P. L. (1994). Factors affecting the strength of alkali-activated slag. Cement and Concrete Research, 24(6), 1033–1043. doi:10.1016/0008-8846(94)90026-4.

[108] Davidovits, J. (1994). High-alkali cements for 21st century concretes. Special Publication, 144, 383-398. doi:10.14359/4523.

[109] Ram, A. K., & Mohanty, S. (2022). State of the art review on physiochemical and engineering characteristics of fly ash and its applications. International Journal of Coal Science Technology, 9, 1-25. doi:10.1007/s40789-022-00472-6.

[110] McGannon, H. E. (1971). The making, shaping and treating of steel. The AISE Steel Foundation, Pittsburg, United States.